IEEE Access
Multidisciplinary ⋮ Rapid Review ⋮ Open Access Journal

Received 22 June 2022, accepted 30 July 2022, date of publication 3 August 2022, date of current version 9 August 2022.

Digital Object Identifier 10.1109/ACCESS.2022.3196037

TOPICAL REVIEW

A Systematic Review on Recent Advancements in Deep and Machine Learning Based Detection and Classification of Acute Lymphoblastic Leukemia

PRADEEP KUMAR DAS[1], (Graduate Student Member, IEEE), DIYA V A[1], (Graduate Student Member, IEEE), SUKADEV MEHER[1], (Member, IEEE), RUTUPARNA PANDA[2], (Member, IEEE), AND AJITH ABRAHAM[3,4], (Senior Member, IEEE)

[1]Department of Electronics and Communication Engineering, National Institute of Technology Rourkela, Rourkela, Odisha 769008, India
[2]Department of Electronics and Telecommunication Engineering, Veer Surendra Sai University of Technology, Burla 768018, India
[3]Machine Intelligence Research Department, Machine Intelligence Research Laboratories, Auburn, WA 98071, USA
[4]Center for Artificial Intelligence, Innopolis University, 420500 Innopolis, Russia

Corresponding author: Pradeep Kumar Das (pdas391@gmail.com)

This work was supported in part by the Analytical Center for the Government of the Russian Federation under Agreement 70-2021-00143 dd. 01.11.2021 and Agreement IGK000000D730321P5Q0002.

ABSTRACT Automatic Leukemia or blood cancer detection is a challenging job and is very much required in healthcare centers. It has a significant role in early diagnosis and treatment planning. Leukemia is a hematological disorder that starts from the bone marrow and affects white blood cells (WBCs). Microscopic analysis of WBCs is a preferred approach for an early detection of Leukemia since it is cost-effective and less painful. Very few literature reviews have been done to demonstrate a comprehensive analysis of deep and machine learning-based Acute Lymphoblastic Leukemia (ALL) detection. This article presents a systematic review of the recent advancements in this knowledge domain. Here, various artificial intelligence-based ALL detection approaches are analyzed in a systematic manner with merits and demits. The review of these schemes is conducted in a structured manner. For this purpose, segmentation schemes are broadly categorized into signal and image processing-based techniques, conventional machine learning-based techniques, and deep learning-based techniques. Conventional machine learning-based ALL classification approaches are categorized into supervised and unsupervised machine learning is presented. In addition, deep learning-based classification methods are categorized into Convolutional Neural Network (CNN), Recurrent Neural Network (RNN), and the Autoencoder. Then, CNN-based classification schemes are further categorized into conventional CNN, transfer learning, and other advancements in CNN. A brief discussion of these schemes and their importance in ALL classification are also presented. Moreover, a critical analysis is performed to present a clear idea about the recent research in this field. Finally, various challenging issues and future scopes are discussed that may assist readers in formulating new research problems in this domain.

INDEX TERMS Acute Lymphoblastic Leukemia, blood cancer, classification, deep learning, machine learning, segmentation.

I. INTRODUCTION

Leukemia is a blood cancer that affects white blood cell (WBC) replication in the bone marrow. It causes an increase in the number of abnormal WBCs, which leads to a decrease in immunity [1]–[8]. WBC is an important component of blood like other two crucial components: Erythrocyte (Red Blood Cell) and platelet [1], [7], [9]–[11]. WBC contains a nucleus and cytoplasm, as presented in Fig.1.

Leukemia is classified mainly into two types: acute and chronic [1], [2], [4], [6], [8], [10]–[12]. Acute Leukemia develops very quickly and gets to the worse stage, whereas chronic Leukemia takes comparably more time to worsen. According to the French-American-British (FAB)

The associate editor coordinating the review of this manuscript and approving it for publication was Gang Mei.

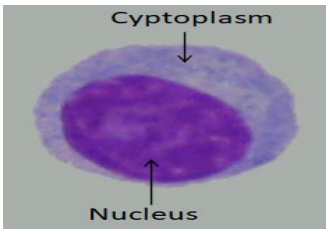

FIGURE 1. Structure of WBC.

classification model, Acute Leukemia is further categorized as ALL and Acute Myeloid Leukemia (AML) [8], [10]–[12]. Similarly, chronic Leukemia is of two subtypes: Chronic Lymphocytic Leukemia (CLL) and Chronic Myeloid Leukemia (CML) [11]. Hence, Leukemia is of four types: ALL, AML, CLL, and CML.

ALL is a fastly growing blood-cancer that severely affects lymphoid progenitor cells in the bone marrow, blood, and extramedullary sites [13]. In ALL, the number of B lymphatic-cells is more than that of T-cells. B-cells are responsible for preventing germs' infection, whereas T-cell kill the infected cells [14].

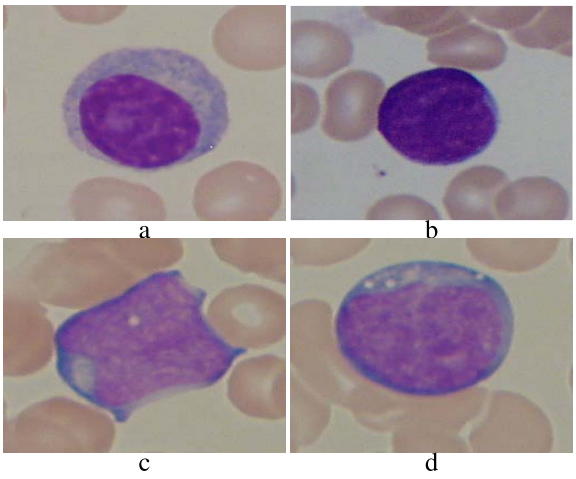

FIGURE 2. Healthy WBC and ALL subtypes: (a) Healthy and (b) L1; (c) L2 and (d) L3 -cells.

According to the FAB model, ALL can further be classified into three subtypes: L1, L2, and L3, as displayed in Fig. 2 [12], [14], [15]. L1 is a small uniform cell with a well-structured nucleus and little cytoplasm. L2 has an irregular nucleus with nonuniform cytoplasm. L3 has a normal shape and size with an oval or round nucleus. It has a fair amount of cytoplasm with vacuoles. It is relatively large compared to L1 [15]. Adults above 50 years and children below five years are in leukemia (ALL) higher-risk group. Early disease diagnosis with appropriate treatment can save the life.

Manual detection of hematological disorders like acute leukemia is required a well-experienced expert physician/doctor for the more accurate early detection. In addition, the complex nature of blood cells, presence of noise, blurring, weak edges, intensity inhomogeneity, cell overlapping make the manual detection using microscopic analysis of blood cells manually very difficult. Manual detection of the hematological disorder is a time taking and error-prone process [1], [2], [4], [6]–[10], [14], [16]–[20]. On the other hand, recent advancements in artificial intelligence techniques like machine learning and deep learning help to design more accurate systems for detecting hematological disorders. In conventional machine learning techniques, crucial hand-crafted features (geometrical, color, texture features along with the features extracted by employing Local Binary Pattern (LBP) [21], Local Directional Pattern (LDP) [22], Discrete Orthogonal S-Transform (DOST) [23], Gray Level Co-occurrence Matrix (GLCM) [24] and Gray Level Run Length Matrix (GLRLM) [25]) are exploited by more efficient classification approaches to predict diseases more accurately. In addition, in preprocessing and segmentation steps, special care should be taken to suppress the above-mentioned issues. However, in deep learning approaches, the extraction of more significant deep features in addition to more efficient classification is performed within a single neural network system for achieving more accurate disease detection by nullifying the effects of noise, blurring, weak edges, intensity inhomogeneity, and cell overlapping up to a great extent. Hence, more efficient computer-aided detection (CAD) systems help in more accurate early detection of disease. It assists the doctor in proper disease diagnosis and treatment planning to save valuable lives.

Computer vision-based systems have been developed in the recent past to detect such hematological disorders. Machine Learning and Deep Learning have emerged as a preferred medical image analysis approach for more accurate disease diagnosis [2], [4]–[11], [14]–[17], [26]–[35]. The basic steps in the conventional machine learning-based detection and classification of Leukemia are: preprocessing, segmentation, feature extraction, and classification, as presented in Fig. 3. Pre-processing is used for improving the image quality. The objective behind segmentation is to extract desired WBCs (by eliminating platelets and RBCs) and separate the overlapped cells [8], [10], [16], [17]. After this, relevant features are extracted, and then a classifier is applied to achieve a more efficient performance. This review article presents a description of each step systematically.

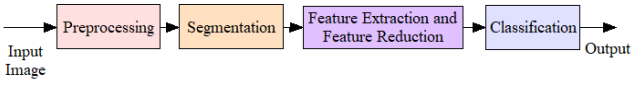

FIGURE 3. Schematic of leukemia detection.

Very few literature reviews on the detection of ALL are available [14], [36]–[38]. In 2016, Bagasjvara *et al.* [36] presented a review on ALL detection in which they have mainly discussed several image processing and classical machine learning-based ALL detection approaches. They have not analyzed deep learning schemes, transfer learning schemes, challenging issues, and future scopes in this

direction. In 2020, Al-Dulami *et al.* [14] and anilkumar [38] have done survey on various segmentation schemes for ALL detection. In both these review works, the authors have emphasized the discussion of several segmentation approaches, whereas they have not focused on classification schemes. They have more concentrated on classical image processing schemes rather than advanced machine and deep learning schemes. In 2020, a brief review work was presented by Parthvi *et al.* [37]. In that review work, they have discussed some popular machine learning and deep learning-based ALL detection approaches. However, they have not discussed advanced deep learning and transfer learning-based ALL detection schemes. More importantly, the reviews are not well structured as systematic categorization of segmentation and classification schemes are absent. Moreover, discussion of machine learning and deep learning schemes, dataset-wise performance analysis of existing schemes, and observations from the study are not presented in that review work.

Hence, it motivates us to present a systematic review of the recent advancements in deep and machine learning-based Acute Lymphoblastic Leukemia (ALL) detection. We give a brief analysis of various segmentation, feature extraction, and classification methods that help researchers get a brief idea about Leukemia detection developments. Moreover, several challenging issues and future scope in this research field are also discussed.

The rest of the paper is structured as follows. Section II, III and IV present an overview of preprocessing, segmentation methods, and feature extraction/ feature selection techniques, respectively. A detailed analysis of machine learning and deep learning-based classification approaches are presented in Section V and VI, respectively. The validation measures are discussed in Section VII, whereas a brief analysis of datasets is illustrated in Section VIII. Section IX emphasizes technical discussion. The critical analysis of the study is presented in Section X. Section XI focuses on various challenging issues, whereas Section XII emphasizes future scopes. Finally, the paper is concluded in Section XIII.

II. PREPROCESSING

The quality of acquired microscopic images relies on camera type, microscope type, light source, capturing camera angle, illumination variation, and noise. Hence, stain normalization is a crucial preprocessing step that normalizes all stain slides to deal with variations in capturing environments, particularly lighting condition variations. It minimizes the illumination and color variations due to different capturing environments of microscopic images taken from different laboratories and thus improving the segmentation and classification performances [39], [40]. A simple way to deal with this issue is histogram equalization or modified versions of it like adaptive histogram equalization [10], [41] and Contrast Limited Adaptive Histogram Equalization [10], [42]. Gehlot *et al.* [40] have presented an efficient coupled self-supervised framework in which two U-Net-type modules are employed. The first module is applied for identity transformation, whereas the second one is used for stain normalization.

The purpose of preprocessing is to improve image quality. It is employed for denoising, deblurring, edge enhancement. For example, Laplacian of Gaussian (LoG), or LoG-based modified high-boosting (LoGMH) operation, is employed for these purposes. Laplacian operation is applied for deblurring and edge enhancement. However, it is noise-sensitive. Thus, in LoG, a Gaussian filter is used before the Laplacian operation for suppressing the noise effect [1], [43]. LoGMH is a modified version of LoG that hybridizes the benefits of LoG with the benefits of high-boosting operation to improve the performance further [1].

Moreover, data augmentation is applied as a preprocessing step in machine learning and deep learning schemes to suppress the overfitting issue. Data augmentation is usually employed in the training phase to enhance training data size by slightly modifying the existing data like padding, re-scaling, horizontal or vertical flip, translation, random rotation, zoom, and crop [2], [6], [7], [44]. Thus, it helps to properly train a system, resulting in improved segmentation or classification performance.

III. SEGMENTATION METHODS

This section describes several segmentation methods that are employed to segment WBCs more precisely. It has an essential role in overall performance and disease diagnosis. The prime objective of segmentation is to extract desired WBCs (by eliminating platelets and RBCs) and separate the overlapped cells. It mainly consists of three types of segmentation approaches: signal and image processing based techniques, machine learning-based techniques, and deep learning-based techniques, as illustrated in Fig. 4. Usually, machine learning and deep learning-based techniques deliver better performance than the first one.

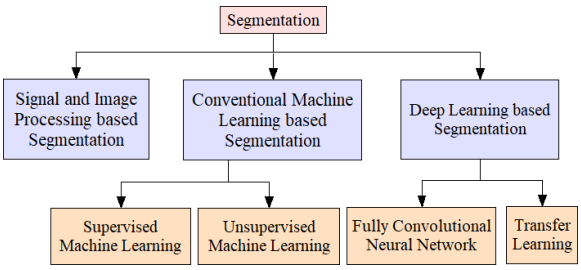

FIGURE 4. ALL segmentation technique.

A. SIGNAL AND IMAGE PROCESSING BASED SEGMENTATION

In this section, we discuss various signal and image processing based WBC segmentation approaches: thresholding-based techniques, morphological operations, watershed-based techniques, circle/ ellipse-fitting-based techniques, active contour/ level set-based techniques. Though our review work emphasizes deep and machine learning-based ALL detection and classification, several signal and image

processing-based conventional segmentation approaches are discussed since these techniques are employed in various machine learning-based classification models whose performances have a significant role in overall classification performance.

Thresholding-based segmentation is the simplest segmentation method. It is suitable when the cells do not touch or overlap one another and have a clear depth difference between objects and background [45], [46]. Selecting an appropriate threshold value is the main challenge, particularly due to the complex nature of cells and intensity inhomogeneities and overlapping cells. Several researchers have applied the Ostu-based threshold method [45]–[47] to segment WBC. Selecting an appropriate threshold value is the main challenge. In 2019, Mishra *et al.* [8] have employed the triangle method for thresholding [48] to extract leukocytes from the background.

Zhao *et al.* [46] have applied morphological operations like erosion and dilation on them, where erosion eliminates insignificant cells, and dilation grows the nucleus of WBCs. Rawat *et al.* [34] used global thresholding and morphological opening techniques for segmentation. Dorini *et al.* [49] used morphological operators and scale-space analysis for the segmentation of WBC cells. But, this gave only qualitative analysis, and chances for misclassification were high. Self Dual Multi-scale Morphological Toggle (SMMT) operator was used by Dorini *et al.* in another paper [50], which gave a more accurate segmented result than the earlier one.

Various researchers have employed the Watershed algorithm to segment overlapped and touched cells [19], [51]. However, it faces an over-segmentation problem due to cells' irregular shape. Some researchers have applied a marker-based watershed algorithm to segment overlapped and touched cells more effectively and solve the above problem [8], [16], [17]. In this technique, we have first extracted the marker, and then the marker is imposed on the gradient to get the segmented cells [8], [16], [17].

Fadhel *et al.* [51] have suggested a circle Hough Transform (CHT)-based technique to segment overlapped cells. They found that it delivers superior performance to the watershed algorithm. It is also faster than the watershed algorithm. However, it is incapable of separating overlapped elongated-cells perfectly. In 2020, Anita and Yadav presented an automated ellipse-fitting-based technique to detect WBCs efficiently [52]. In 2021, Das *et al.* [1] have suggested a hybrid ellipse-fitting model by integrating the advantages of algebraic and geometric ellipse-fitting methods to yield promising segmentation for the detection of AML, ALL, and sickle-cell disease. Despite it giving a promising ellipse fitting performance, it is unable to demonstrate excellent cell-segmentation performance with accurate boundary detection as normally, cells are not perfectly elliptical.

Active contour and level set-based methods are employed to detect object boundaries properly and to achieve efficient segmentation [53]–[57]. Contours are object boundaries that define regions of interest [53], [57]. Emo *et al.* [54] have employed a region-based active contour model for effective segmentation of WBCs. However, an active contour suffers from yielding perfect segmentation since it cannot manage topological variations: splitting and merging [55], [56]. The level set method is introduced to overcome this limitation and able to represent the contour of complex topology [55], [56]. Khadidos *et al.* [56] have suggested a novel weighted level set method to deliver more accurate medical image segmentation.

However, most of the signal and image processing-based methods are unable to deliver more accurate segmentation due to the complex nature of cells, intensity inhomogeneities, and overlapping cells. Moreover, more accurate segmentation can be achieved by hybridizing a recent active contour/ level set method with the marker-based watershed algorithm. It is one of the future scopes in this field.

B. CONVENTIONAL MACHINE LEARNING BASED SEGMENTATION

The conventional machine learning-based segmentation method is broadly classified into two types: supervised and unsupervised. The details about these machine learning techniques are discussed in Section IV. This section analyzes the recent machine learning algorithm-based WBC segmentation approaches that have an essential role in ALL detection and classification.

1) SUPERVISED MACHINE LEARNING-BASED SEGMENTATION

Supervised machine learning is a learning algorithm that trains the machine using labeled data. Support vector machine (SVM) [58], Artificial Neural Network (ANN) [59], [60], and Random Forest [61] are more popular supervised learning techniques.

Abdulhay *et al.* [62] have employed SVM to segment WBC efficiently. Mohapatra *et al.* [63] have suggested a Functional Link ANN (FLANN)-based WBC segmentation approach. FLANN is a type of ANN that has a flat network with no hidden layer [63]–[65]. It can solve the non-linear problem better than the single-layer perceptron [63]. They treat the segmentation as a pixel classification problem and segment the nucleus, cytoplasm, and background quite effectively.

2) UNSUPERVISED MACHINE LEARNING-BASED SEGMENTATION

Unsupervised machine learning is a learning algorithm that trains the machine using unlabeled/ unclassified data. The unsupervised model works on its own to extract the features and information without knowing the labeled/ class of the data. K-means clustering [66], [67] and Fuzzy C-means clustering (FCM) [68] are the two most popular unsupervised machine learning-based techniques. The objective of these clustering techniques is to obtain similar regions (clusters) within the input image.

Several researchers have employed the k-means clustering technique to segment WBCs efficiently, which has a vital

role in ALL detection and classification [10], [11], [18], [29]. In 2020, Das *et al.* [10] have suggested a k-means based color segmentation technique to extract WBC successfully. On the other hand, Acharya *et al.* [69] have applied the k-medoid-based segmentation approach to separate cytoplasm from the nucleus. Though the k-medoid technique is slower than the k-means, it achieves better segmentation performance and more robust than k-means [69].

Mohapatra *et al.* [70] have employed FCM to segment WBCs successfully. Since the FCM-based segmentation depends on similarity criteria, it is prone to noise and intensity inhomogeneity. Hence, it can't achieve more accurate segmentation, especially in the presence of noise and intensity inhomogeneity [9], [71]. Chung *et al.* [71] have suggested an improvised FCM that modifies membership functions depending on spatial information to overcome the limitation. Mohapatra *et al.* [72] have suggested a rough fuzzy c-mean clustering-based WBC segmentation approach. It boosts the segmentation performance by updating fuzzy membership value depending upon cluster mean, unlike FCM. They have observed that it outperforms k-means, k-medoid, FCM, and rough c-means. MoradiAmin *et al.* [33] have applied FCM to extract the nucleus of WBC. Jha and Dutta [73] have suggested a hybrid WBC segmentation approach. It combines the segmentation outputs of active contour and FCM to achieve more efficient segmentation.

C. DEEP LEARNING-BASED SEGMENTATION

Recent advancement in deep learning makes it a preferred approach for image segmentation. Here, two major types of deep learning-based segmentation schemes used in ALL detection and classification, i.e., traditional deep learning-based segmentation and transfer learning-based segmentation approaches are discussed. The details about the deep learning techniques are briefly analyzed in Section VI.

Wang *et al.* [74] have suggested a CNN-based WBC detection technique using a single shot multi-box detector [75] and a modified You Only Look Once (YOLOv3) [76]. Mandal *et al.* [77] have presented a U-Net [78] based semantic segmentation to detect overlapped nuclei. Shahin *et al.* [79] have presented a transfer learning-based segmentation/detection approach. Shahin *et al.* [79] have presented three deep learning methods to classify five types of WBCs: Monocyte, Lymphocyte, Basophil, Eosinophil, and Neutrophil. Shahin *et al.* [79] have suggested a new CNN model (WBCsNet) to detect WBCs more accurately. It contains 3 convolution layers, 2 pooling layers, 4 activation (ReLu) layers, 2 fully connected layers, followed by a softmax layer.

Automated and more precise nuclear segmentation has an important role in improving overall classification and disease detection performances [80]–[83]. Duggal *et al.* [80] have recommended deep belief network-based segmentation schemes to detect nuclei of WBCs more accurately.

Roy and Ameer [84] have suggested a transfer learning-based semantic segmentation approach to yield more accurate WBC segmentation. They have applied DeepLabV3+ [84] to achieve more precise semantic segmentation, where ResNet50 [85] is used as the segmentation model.

IV. FEATURE EXTRACTION AND FEATURE REDUCTION

In this section, we discuss several feature extraction and feature reduction approaches that are applied to extract significant features that have an essential role in ALL detection and classification. We broadly divide the feature extraction into two types: (i) conventional feature extraction; (ii) machine learning and deep learning-based feature extraction. Usually, feature extraction is followed by a feature reduction technique to select more significant features. Principal Component Analysis (PCA) [86], Probabilistic Principal Component Analysis (PPCA) [87], and Linear Discriminant Analysis (LDA) [88] are some popular feature reduction techniques, which are applied to improve the overall performance and make the system computationally efficient.

A. CONVENTIONAL FEATURE EXTRACTION

Here, we discuss geometrical-, color-, and statistical-texture-features. Moreover, extraction of important texture-fearures by applying Local Binary Pattern (LBP) [21], Local Directional Pattern (LDP) [22], Discrete Orthogonal S-Transform (DOST) [23], Gray Level Co-occurrence Matrix (GLCM) [24] and Gray Level Run Length Matrix (GLRLM) [25] are also analyzed.

Several researchers have extracted crucial geometrical, color, and statistical texture features to yield efficient ALL classification [10], [18], [20], [29], [29], [34], [45], [57], [89], [89]. Moshavash *et al.* [19] have extracted LBP-based texture-features along-with geometrical and color features to classify ALL efficiently. Jha and Dutta [73] have applied LDP to extract efficient texture features. Das *et al.* [10] have extracted vital geometrical features: perimeter, area, rectangular bounding-box, minimum bounding-ellipse, convex hull, and circularity. They have extracted histogram-based color features. Moreover, they have suggested GLCM and GLRLM-based feature extraction technique to extract important texture features. They have presented a PCA-based feature selection. Mishra *et al.* [17] have presented GLCM-based feature extraction followed by a PPCA-based feature selection method to classify malignant and benign. Mishra *et al.* [8] have used DOST for feature extraction, whereas a hybrid of PCA and LDA techniques is applied for feature reduction.

B. MACHINE LEARNING AND DEEP LEARNING-BASED FEATURE EXTRACTION

Machine learning and deep learning methods, particularly transfer learning-based methods, are widely employed to extract more significant features, which play a key role in ALL classification.

Vogado *et al.* [35] have presented VGG-f [90]-based feature extraction followed by PCA-based feature reduction

techniques to extract crucial features. Finally, they have used an ensemble classifier to classify benign and malignant efficiently. Vogado *et al.* [4] have applied AlexNet [91], CaffNet [92], VGG-f [90] to extract efficient features. Then, they have used gain-ratio to select more important features.

Shahin *et al.* [79] have suggested a transfer learning-based feature extraction scheme, where they have applied OverfeatNet [93], AlexNet [91], and VGGNet [90] for feature extraction. Then, they have used Chi-squared or PCA-based feature selection followed by SVM-based classification. In 2021, Das *et al.* [6] have extracted essential features by utilizing the best training model from the three modified ResNet models presented by them. In 2022, Das *et al.* [5] have recommended a MobileNetV2-SVM framework in which MobileNetV2 is employed for feature extraction, whereas SVM is used for efficient classification.

V. CONVENTIONAL MACHINE LEARNING-BASED CLASSIFICATION

In this section, we discuss various conventional machine learning based ALL classification approaches. Machine learning is a sub-branch of Artificial intelligence, which uses logical, statistical, and mathematical techniques to help a machine learn from data without programming and from a general principle of conclusion using data samples. That is, a computer learns from its own experience by using the technique of artificial intelligence in pattern recognition. Thus, the conclusions are mainly based on the data that we have prior to the process. Usually, machine learning-based ALL classification is either supervised or unsupervised, as shown in Fig. 5. However, some researchers have suggested ensemble or hybrid classifiers by combining the benefits of more than one classifiers (supervised or unsupervised) or single classifier with different kernels and parameters to boost the performance. Here, we discuss all these techniques.

A. SUPERVISED MACHINE LEARNING

Supervised machine learning is a learning algorithm that requires labeled data to properly train the algorithm for yielding more efficient classification. This section describes some popular supervised learning techniques: k-nearest neighbor (k-NN) [94], Naive Bayesian Network [95], Multi-Layer Perceptron (MLP) [96], Decision tree [97], Random Forest [98], Support vector machine (SVM) [58], Artificial Neural Network (ANN) [59], [60], which are employed for automatic ALL classification.

1) K-NEAREST NEIGHBOUR

The distance between two data samples is used for their classification or, in general, based on the nearest neighbors, the decision is taken. Hence, the distance between identical or similar data samples will be less than that of two separate data samples [26], [94], [94], [99]. K-NN usually employs Euclidean distance to chose the nearest neighbor and assigns the respective class. Though KNN is easily implementable, it becomes slower in large datasets, and it is also sensitive to irrelevant parameters [100], [101]. Umamaheswari *et al.* [47] and Madhloom *et al.* [102] have applied KNN for effective ALL classification.

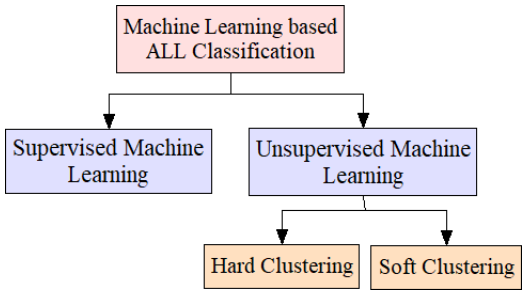

FIGURE 5. Machine learning-based ALL classification.

2) NAIVE BAYESIAN

It is a standard supervised classifier in which the relationship between variables is described using statistics, and more specifically, the probabilities of features are made use of [26], [95], [99]. Thus, rather than predictions, projections of likelihood are made for the classification. In graph theory, the variables are represented using graph nodes, and the relationship between these variables is represented using arcs. In the Naive Bayesian network, there will be only one parent and several children who are independent of each other [26], [95], [99]. Naive Bayes is computationally efficient both in the training and testing phase. During the estimation of probabilities, it ignores the missing values. Hence, the final decision is not affected by these missing values, which makes it more robust [99]. Sabino *et al.* [103] have applied Naive Bayesian to classify Leukemia and five sub-types of healthy WBCs: Basophil, Neutrophil, Eosinophil, monocyte, and lymphocyte.

3) MULTI-LAYER PERCEPTRON (MLP)

MLP is a class of feed-forward ANN. It consists of multiple layers of perceptrons (with threshold activation). An MLP contains at least three layers of nodes: an input layer, a hidden layer, and an output layer. Every node except input nodes is a neuron that employs a nonlinear activation function. MLP uses a supervised learning approach called backpropagation for proper training. Its multiple layers and nonlinear activation differentiate it from linear perceptron [96], [104], [105]. Multiple inputs are weighted in a perceptron, then an activation function is applied, and a single result is produced at the output [96], [104], [105]. Mathematically it is presented as:

$$y = \phi(\sum_{i=1}^{m} w_i x_i + b) \tag{1}$$

where, x is an input-vector, y is the output, w is the perceptron's weight vector, and b is the bias term. The activation function, ϕ, is a nonlinear function like sigmoid. Nazlibilek *et al.* [104] have applied MLP to achieve efficient WBC classification, whereas Neoh *et al.* [105] have used MLP to classify ALL effectively.

4) DECISION TREE

As the name implies here, the data is represented in a tree format; data sample labels as leaf nodes, and various characteristics as internal nodes. Hence, Decision Tree (DT) is basically follows a divide and conquer method for the classification purpose [26], [97], [99], [106].

In this scheme, a complex decision is divided into the integration of various simpler decisions [107]. In DT, each link is mutually distinct as well as exhaustive. A particular pattern's classification begins from a root-node that focuses on a certain pattern's property [108]. Different links are connected to descendent nodes based on various possible values. Then, a decision at the new node (descendent node) is taken by treating it as the root of a subtree. This process will stop when a leaf-node is reached [108].

A commonly used algorithm for decision tree classification is C4.5 [109], [110]. EC4.5 [109] is a robust variant and 5 times better than C4.5 [111] but has the same decision tree as that of C4.5. The training stage is faster than a neural network, but it has no flexibility for modeling parameters [100]. Negm *et al.* [29] have employed a decision tree to achieve efficient ALL classification. Ke *et al.* [112] have proposed a Gradient Boosting Decision Tree-based classifier known as LightGBM to yield efficient classification. Mandal *et al.* [31] have employed the LightGBM model [112] to classify Leukemia efficiently. They have observed that it gives better performance than SVM.

The main disadvantage of DT is that a single tree provides the prediction, which makes it noise-sensitive [113]. Moreover, a smaller data variation needs a lot of changes to produce an optimal DT structure, thus making it comparatively unstable. Its performance can be boosted by efficiently combining predictions of various trees [113].

5) RANDOM FOREST

Random forest (RF) is a more accurate, powerful, and widely used Machine learning algorithm [61], [98]. It is a tree structure-based classifier in which every tree depends on a random vector's value and the distribution of trees in the forest [61], [98]. Its output (class of an object) is predicted effectively by integrating the predictions of all the DTs.

Mishra *et al.* [17] have used an RF classifier to classify lymphoblasts into benign and malignant. In 2019, Mishra *et al.* [8] presented an Adaboost-based RF (ADBRF) for ALL classification. In ADBRF, RF [98] act as a base classifier, whereas Adaboost [114] is an ensemble learning technique employed to enhance prediction performance.

6) SUPPORT VECTOR MACHINES (SVM)

SVM is one of the most popular supervised machine learning technique, widely used in machine learning for regression and classification [58], [115]. It separates various classes using hyperplanes. Its objective is to maximize the distance between the hyperplane and every feature vector in such a way that each feature-vector feels safe in the classification point of view. This can be achieved only when it satisfies:

$$y_i \left(w.x_i \dot{+} b\right) \geqslant 1 \tag{2}$$

where x_i represents an input feature vector and y_i denotes the corresponding label or class belongingness. The feature vector x_i is called support vector only if $y_i \left(w.x_i \dot{+} b\right) = 1$. It has the most accurate performance when the data is linearly classifiable. It actually converts a nonlinear problem into a linear separation problem and thus leads to an easier classification. To classify non-linearly separable data, mapping the data into a higher-dimensional space can be made use of. The selection of correct kernel function and parameters is crucial in that case [26], [58], [100], [115]. Most of the researchers use Radial basis functions (RBFs) as the kernel functions to map the data into higher dimensional space [26], [100].

Various researchers have suggested SVM-based ALL classification techniques to classify benign and malignant efficiently [4], [10], [11], [14], [16], [31], [33], [34], [45], [70]. MoradiAmin *et al.* [33] have employed an ensemble of SVM classifiers with various kernels and parameters to classify three ALL subtypes: L1, L2, L3, and healthy WBC successfully. Its amazing generalization ability, discriminative power, and optimal solution make it a preferred machine learning technique [100].

7) ARTIFICIAL NEURAL NETWORKS (ANNs)

Artificial neural networks (ANNs) are one of the most popular neural network-based classifiers. It is similar to the network of neurons found in the human brain [59], [60]. It estimates output from a large number of input data. ANN can be supervised, unsupervised, or reinforcement machine learning technique depending on the training process and learning rule. A back-propagation neural network (BPNN) is a popular supervised ANN, whereas a self-organizing map (SOM) is a popular unsupervised ANN. In supervised ANN, the backpropagation algorithm boosts the learning ability of ANN by comparing the produced output to the desired output. Thus, it optimizes the error [26], [59], [60], [116]. Generally, an ANN comprises an input layer, one or more hidden layers, and an output layer. A sum of weighted inputs and bias terms is applied to a non-linear unit (activation function). An activation function helps the NN to learn complex patterns and predict the desired output. The significant feature of an effective activation function is its ability to add nonlinearities into a NN. Sigmoid, Tanh, ReLU, and Softmax are some popular nonlinear activation functions.

ANN can be a feedforward or feedback neural network. In MLP, no recurrent connection exists, whereas, in ANN, there may have recurrent connections or may not. Parameter sharing is not occurred in MLP, whereas in some specific types of ANN like CNN, parameter sharing is performed.

Negm *et al.* [29], Acharya *et al.* [69], and Al-jaboriy *et al.* [117] have employed ANN to achieve efficient ALL classification. Mohapatra *et al.* [63] have applied Functional Link ANN (FLANN) to classify ALL effectively. FLANN is a type of ANN that has a flat network having no hidden

layer [63]–[65]. In this network, nonlinearity is added by improving input patterns with nonlinear functional expansion. Nonlinear functional expansions like polynomial and trigonometric enhance the dimensionality of an input vector, resulting in improved discrimination capability. Appropriate selection of functional expansion has an important role in the overall performance of FLANN [63]–[65].

B. UNSUPERVISED MACHINE LEARNING

Unsupervised machine learning is a learning algorithm that trains the machine using unlabeled/ unclassified data. The unsupervised model works on its own to extract the features and information without knowing the label/ class of the data. Clustering is a widely used unsupervised machine learning technique. Its objective is to decide the class belongingness based on similarities between objects. There are mainly two types of clustering: hard clustering and soft clustering.

1) HARD CLUSTERING

Hard clustering is a type of clustering where each data strictly belongs to one class like in K-means and K- medoid.

a: K-MEANS

K-Means clustering is an unsupervised method that decides a pixel or object's class belongingness based on the nearest mean [9], [10], [66], [67]. Algorithm 1 presents the k-means clustering algorithm. It minimizes the objective function to make it more suitable for convex clusters. However, it is not preferable for arbitrarily shaped ones [72].

Algorithm 1 K-Means Clustering

Input: Input data (Images)
Output: Resultant clusters
Begin
1: Choose the number of clusters, K
2: Generate K clusters. Select K centroid points randomly or using an effective heuristic scheme.
3: Update every cluster by allotting each data-point to the respective cluster based on the centroid of a cluster near to it.
4: Compute the centroid of all updated cluster (group).
5: Estimate the distance between every data point and every cluster centroid.
6: Update every cluster by allotting each data-point to the respective cluster based on the centroid of a cluster near to it.
7: Repeat step-4 through step-6 till convergence of the algorithm (i.e., when we get a difference between two consecutive means less than a threshold for all clusters or we reach the predefined number of iterations).
End

Usually, it is preferred for segmentation and classification tasks where the available data is unlabeled. Other more efficient supervised schemes are preferred over it while labeled data is present due to their superior performance as they are efficiently trained using the labeled data.

Laosai *et al.* [18] have applied the k-means clustering technique to classify acute Leukemia. It effectively classifies healthy, AML, and ALL with approximately 97% accuracy.

b: K-MEDOID

Similar to k-means, k-medoid optimizes the squared error. However, in k-medoid, the most centrally located datapoint (from the given datapoints) is selected as cluster-center, known as medoid. Hence, it has more immunity to noise and outliers; thus much better than K-Means [72], [118].

2) SOFT CLUSTERING

Soft clustering is a type of clustering technique, where data may belong to more than one clusters. Here, we discuss some popular soft clustering methods: Fuzzy C-Means (FCM) [68], Rough C-Means (RCM) [119], and Rough-Fuzzy C-Means (RFCM) [119].

a: FUZZY C-MEANS CLUSTERING (FCM)

FCM is a popular unsupervised learning method [68]. In 1973, the first soft partitive algorithm was developed by Dunn and then got improved into the FCM. A fuzzy membership function is used to estimate the degree of belongingness of an object/ pixel corresponding to a cluster [68], [72]. An objective function is also formed, which should be optimized to form the partitive matrix. It is mathematically represented as:

$$Z = \sum_{i=1}^{N}\sum_{j=1}^{M}(\mu_{ji})^n \|X_i - c_i\|^2 \tag{3}$$

where c_i is the jth cluster centre, $1 \leq n < \infty$ is the degree of fuzziness, $\|.\|$ is the euclidean distance norm, and $\mu \in [0, 1]$ is the membership function of the ith data pattern to it. We have the equation for c_i and μ_{ji} as,

$$c_i = \frac{\sum_{i=1}^{N}(\mu_{ji})^n X_i}{\sum_{i=1}^{N}(\mu_{ji})^n} \tag{4}$$

$$\mu_{ji} = \frac{1}{\sum_{k=1}^{M}(d_{ji}/d_{ki})^{2/(m-1)}} \tag{5}$$

where,

$$d_{ji} = \|X_k - c_i\|^2 \tag{6}$$

Viswanathan *et al.* [120] have suggested an FCM-based ALL classification approach.

b: ROUGH C-MEANS (RCM)

By considering each class as a rough set, the idea of K-Means is extended into RCM [72], [119]. The lower and upper approximations of a rough set X is given by $\underline{B}X$ and $\overline{B}X$, respectively. Objects in a rough set are classified into lower approximation if it clearly satisfies a given vague definition,

whereas it is classified into upper approximation if satisfying the definition is still ambivalent. These two approximations result in objects in rough boundaries [72]. RCM can be completely defined depending upon the weight factors (W_{low}, W_{up}) and the threshold (T). T is the relative distance between data and cluster centroids. Tuning of these parameters is crucial for the segmentation process [72], [119].

c: ROUGH-FUZZY C-MEANS (RFCM)

RFCM was developed by integrating the FCM concept into the RCM to boost the performance [72], [119]. By using the membership function, we can actually segment an image, where the membership value μ_{ji} of a data sample X_i is integrated into the cluster mean c_j relative to all other means c_i. There is no need to use the Euclidean distance d_{ji}. A better segmentation accuracy is achieved by incorporating fuzziness into RCM [72], [119].

Unsupervised learning techniques don't need labeled data to classify data/ objects efficiently. However, the selection of an appropriate number of clusters to yield excellent performance is still challenging.

C. ENSEMBLE CLASSIFIER

An ensemble classifier can be developed by using more than one classifiers or using a single classifier with different kernel functions and parameters. It is used to improve classification performance by combining the benefits of multiple classifiers or the benefits of multiple kernels [121]. Adaboost is an example of an ensemble classifier that combines classifiers of the higher error rate to produce a classifier of lower error rate [8], [114]. Mohapatra *et al.* [121] have presented an ensemble classifier (ensembles of KNN, MLP, and SVM classifiers) to classify malignant and benign. They observed that it outperforms KNN, MLP, and SVM since it retains these three methods' benefits. However, it has also become computationally expensive. Moshavash *et al.* [19] have suggested two ensemble classifiers: Ensemble1 (ensemble of KNN, Decision tree, SVM, and NaiveBayes classifiers) and Ensemble2 (it is developed by using five SVM kernels: polynomial, linear, Gaussian radial basis, multi-layer perceptron, and quadratic).

In 2019, Mishra *et al.* [8] presented an Adaboost-based RF (ADBRF) for ALL classification. In ADBRF, RF [98] acts as a base classifier, whereas Adaboost [114] is an ensemble learning technique employed to enhance prediction performance. Hence, the combination of RF (as a weak learner) and Adaboost yields better performance. Vogado *et al.* [35] have applied an ensemble of three classifiers (Multilayer Perceptron, SVM, and Random Forest) to classify benign and malignant efficiently. MoradiAmin *et al.* [33] have employed an ensemble of SVM classifiers with various kernels and parameters to classify three ALL subtypes: L1, L2, L3, and healthy WBC successfully. Though the ensemble classifier yields superior performance than the employed individual classifier, it becomes computationally slow.

D. HYBRID CLASSIFIER

In the testing phase of a hybrid classifier (a hybrid of two classifiers), the second classifier executes only for a specific situation (if the first classifier yields poor performance than a predefined label). Thus, it is faster than an ensemble classifier. Hyperrectangular composite neural networks (HRC-NNs) is a hybrid combination of neural networks with a rule-based approach. It consists of crisp if-then rules [89], [122]. Su *et al.* [89] have applied HRC-NNs to classify WBCs effectively.

VI. DEEP LEARNING-BASED CLASSIFICATION

Medical image analysis using deep learning methods is getting remarkable attention because of its efficient performance [2], [4]–[7], [26], [27], [123], [124]. Here, we discuss three types of deep learning-based classification methods: Convolutional Neural Network (CNN), Recurrent Neural Network (RNN), and the Autoencoder, as shown in Fig. 6. CNN is further subdivided into conventional CNN and Transfer learning.

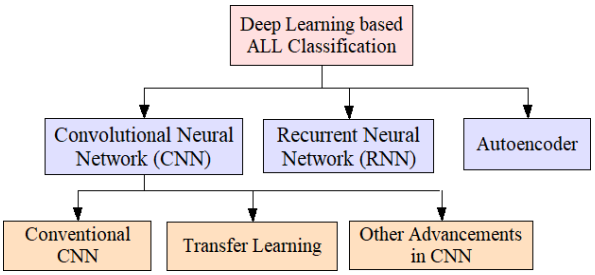

FIGURE 6. Deep learning-based ALL classification.

A. CONVOLUTIONAL NEURAL NETWORK (CNN)

CNN is the most popular deep learning scheme. It is a Neural Network with multiple layers, and it resembles the visual cortex. It works better for correlated multidimensional data inputs like images and thus helps to get the most relevant features out of it without correlation. In CNN, weights are shared adaptively to perform convolution operations on an image, unlike MLP [27].

1) CONVENTIONAL CONVOLUTIONAL NEURAL NETWORK (CNN)

In conventional CNN, convolution layers extract generic features, whereas the deeper layers are incorporated with target-specific features. Hence, features are gradually transformed from generic to target specific [125]. It consists of various layers: an input layer, convolutional layer, pooling layer, fully connected layer, and a classification layer, as displayed in Fig. 7.

a: INPUT LAYER

In this layer of a CNN model, inputs (images) are given. Here, the size of the inputs is also defined.

b: CONVOLUTION LAYER

As its name signifies, a convolution operation is performed in this layer. It is done by performing a dot multiplication

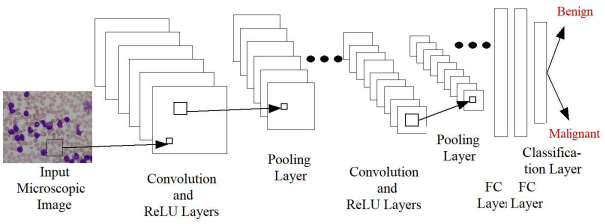

FIGURE 7. Conventional CNN architecture.

between kernel pixels with the respective image pixels on which the kernel pixel is currently lying and then adding all these results to evaluate a convolution output at a particular pixel. Then, the kernel slides over the whole image based on the predefined stride. The objective of this layer is to extract the different features from its previous layer [26].

c: ReLu LAYER

ReLu stands for Rectified Linear Unit. This layer is employed to enhance non-linearity in the CNN model. Here, ReLU activation functions are employed to add nonlinearity instead of traditional tanh or sigmoidal activation functions [91]. ReLU does not saturate near 1, unlike these two functions. More importantly, it makes the network faster with maintaining similar accuracy by improving the learning speed [26], [91]. It is a popular activation function since it is easy to use and is successful at eliminating the drawbacks of other formerly well-liked activation functions.

d: POOLING LAYER

Pooling or sub-sampling is done to reduce the dimensionality of the image, which decreases the image's feature dimension to minimize the computational cost and make the learning faster. It is also used to suppress over-fitting issues. In CNN, Max Pooling and Average Pooling are two popular methods of pooling [26].

(i) Max Pooling: It gives the maximum value from the region of the image upon which the pooling kernel is applied. Its job is to suppress the noise by rejecting all the noisy activations, as well as reduce the dimensionality [26].

(ii) Average Pooling: It gives the mean of the values from the region of the image upon which the pooling kernel is applied [26].

e: FULLY CONNECTED LAYER

A number of fully connected layer(s) is added after the convolutional and pooling layers in the CNN model. As the name implies, every neuron in this layer connects to every neuron of the previous layer. This layer integrates all of the information that the earlier layers had learned to detect the larger patterns. The final fully connected layer integrates information (features) for image classification. Thus, the output size of the final fully-connected layer is selected the same as the number of classes that we intended to classify the input data. SoftMax activation is usually employed in the final fully-connected layers to determine probabilities of class belongingness [26].

f: CLASSIFICATION LAYER

It is the last layer in the CNN model, which exploit the probabilities estimated by the SoftMax activation function for every input to predict the class effectively [26].

Banik *et al.* [3] have recommended a CNN-based ALL classification method. In this method, the first and last layer features are combined. The dropout layer is used to avoid overfitting. In 2020, Jha and Dutta [73] presented a Chronological Sine Cosine Algorithm (SCA)-based deep CNN model to classify ALL successfully. Shahin *et al.* [79] have proposed a new CNN-based framework (WBCsNet) to classify WBC efficiently. Claro *et al.* [126] have suggested a deep-learning network (Alert-Net). It consists of 5 convolution layers, two fully connected layers, and a softmax layer.

Conventional CNN needs a huge dataset to achieve outstanding performance. Since publicly available standard medical datasets are in small size, it is unable to properly fine-tune the weights to extract more important target-specific features efficiently. Thus, it yields relatively poor performance.

2) TRANSFER LEARNING

Recently, transfer learning emerges as a rapidly growing approach in the medical imaging field due to its excellent performance [4], [27], [79], [126]. Transfer learning has the advantage that it does not require a large dataset for the training purpose since it makes use of a pre-trained network and transfers its knowledge or weights to the target-domain tasks (medical imaging tasks). Hence, in the target-domain, only fine-tuning of these pre-trained networks are required. Thus, it yields outstanding performance even for small datasets [4], [27], [79], [126]. Here, we discuss some popular transfer learning approaches: AlexNet [91], CaffNet [92], VGGNet [90], GoogLeNet [127], ResNet [85], MobileNet [128], MobileNetV2 [129], and Xception [130].

a: AlexNet

AlexNet is a famous transfer learning technique. It was developed by Krizhevsky *et al.* [91] in 2012. It has five convolution layers and three fully connected layers, as displayed in Fig. 8. Each convolution layer is followed by ReLU activations (add nonlinearities) and a max-pooling layer (reduce over-fitting) [4], [57], [84], [91].

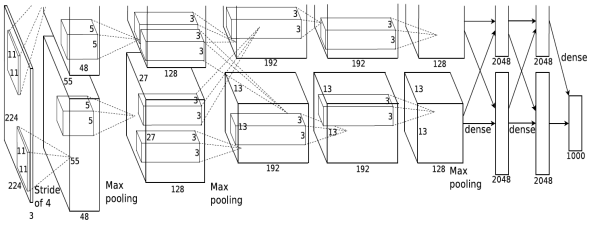

FIGURE 8. AlexNet architecture [91].

b: CaffNet

It was created by Berkeley Vision and Learning Center(BVLC). Similar to AlexNet, it has five convolutional layers and three fully connected layers. It differs from AlexNet in terms of an order of pooling layer and normalization [4], [92].

c: VGGNet

It became popular in 2014 because of its uniform architecture (stuck to a filter-size 3 × 3). Here, a block of filters is employed instead of a convolution layer. It boosts non-linearities and optimizes the receptive field by employing 3 × 3 convolutions in succession, as presented in Fig. 9. The succession of two 3 × 3 and three 3 × 3 convolution layers produce receptive fields of 5 × 5 and 7 × 7 convolution layers, respectively. VGGNet deals with around 138 million amount of parameters. VGG16 and VGG19 have 16 and 19 weighted layers, respectively [90].

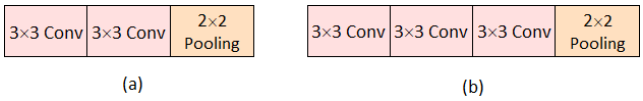

FIGURE 9. Convolution blocks: (a) Block with two 3 × 3 convolution-layers, (b) Block with three 3 × 3 convolution-layers.

d: GoogLeNet

Szegedy *et al.* [127] have presented a novel GoogLeNet architecture that uses an inception module for dimensionality-reduction. The inception module uses a convolutional block that has various filter sizes. The inception module is presented in Fig. 10. As presented in Fig. 10 (b), an efficient inception module is suggested in GoogLeNet architecture [127]. It becomes computationally efficient by applying 1 × 1 convolutions prior to 3 × 3 and 5 × 5 convolutions that yield bottleneck architecture.

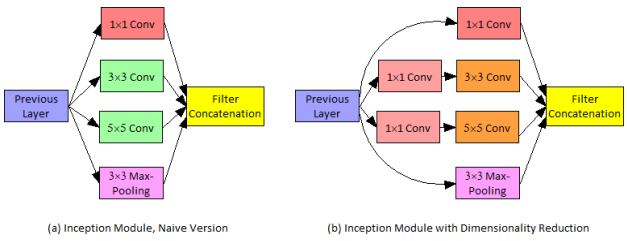

FIGURE 10. Inception module.

e: ResNet

ResNet was created by He *et al.* [85] in 2015, a very deeper network due to many layers. They have recommended skip-connection to overcome vanishing gradient issues, which gives an alternative gradient flow path, as shown in Fig. 11.

The residual factor, $F(x)$ is presented as:

$$F(x) = H(x) - x \tag{7}$$

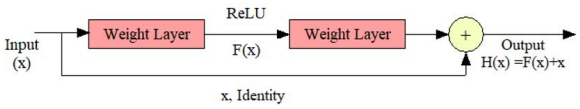

FIGURE 11. Residual learning block.

where, x and $H(x)$ symbolize the input and oupt of the residual block, respectively.

More importantly, in this model, they have recommended learning of residual factor, $F(x)$, instead of the residual block output, $H(x)$, resulting in faster learning and a faster system as $F(x)$ is very small compared to H(x).

f: MobileNet

Wang *et al.* [128] have created a lightweight MobileNet architecture. Depth-wise separable convolution is achieved by applying depth-wise convolution before point-wise convolution to make the system computationally efficient, as shown in Fig. 12. In depth-wise convolution, convolution is individually performed on every input channel. Point-wise convolution is responsible for combining the outputs of depth-wise convolution linearly. They have introduced width and resolution multipliers to make the model faster [128]. Moreover, width is employed for efficiently producing a thicker/ thinner network [128].

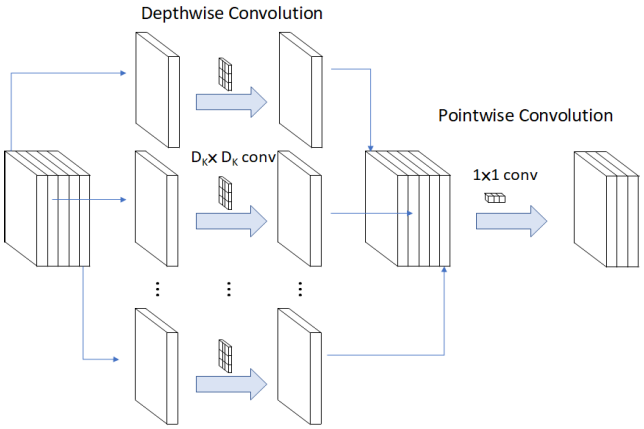

FIGURE 12. Depth-wise separable convolution [128], [129].

g: MobileNetV2

It is a modified version of the MobileNet model, where inverted residual bottleneck structure is introduced. It also uses depth-wise separable convolutions, width, and resolution multipliers to make the model computationally fast [129]. In this architecture, two blocks: MobileNetV2 block 1 (MVB1) and MobileNetV2 block 2 (MVB2), are suggested to make the faster as well as to improve the performance, as presented in Fig. 13 [129]. As displayed in Fig. 13 (a), MVB1 represents an inverted-residual-bottleneck-structure with stride 1, where a skip connection is provided between two bottleneck layers. Hence, it integrates the benefits of both bottleneck and residual structure [129].

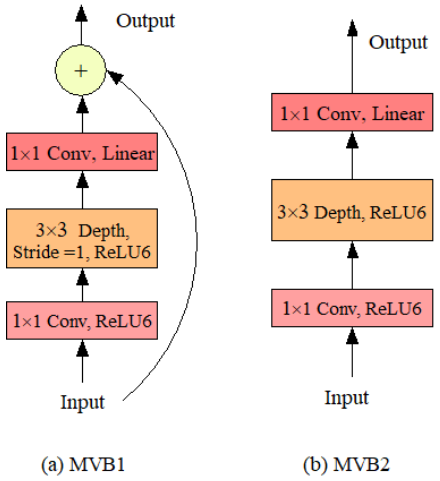

FIGURE 13. MobileNetV2 blocks: (a) MVB1 and (b) MVB2.

Ontheotherhand, MVB2 represents a bottleneck structure with stride $S = 1$ or 2 [129].

h: XCEPTION

Xception is a depth-wise separable convolution-based transfer learning method. It consisting of 14 modules and contains 36 convolution layers in total. All of these modules, except the first and last modules, have linear residual-connections [130].

i: ShuffleNet

Zhang *et al.* [131] have recommended a lightweight faster ShuffleNet framework in which group convolution is also employed on 1×1 layers. The main novelties of this model are the introduction of the ShuffleNet unit and Channel shuffle for group convolutions to make the model faster. ShuffleNet unit exploits channel shuffling to produce a faster transfer learning model [7], [131]. Moreover, it also boosts the performance by sharing information among groups because of channel shuffling.

Shafique and Tehsin [15] have employed AlexNet [91] to classify WBCs into four classes: healthy, L1, L2, L3. It not only classifies healthy and ALL but also efficiently classify three subtypes of ALL. Yu *et al.* [30] have presented an ensemble transfer-learning-based ALL detection approach. They have ensembled VGG-16 [90], InceptionV3 [127], VGG-19 [90], ResNet50 [85], and Xception [130] to classify WBCs effectively. Shahin *et al.* [79] have applied fine-tuned LENet [132] and AlexNet [91] for efficient WBC classification.

Mallick *et al.* [133] have presented five-layered deep CNN-based ALL and AML classification model. Roy and Ameer [84] have used AlexNet [91] to classify subtypes of WBC successfully. Claro *et al.* [126] have presented a deep-learning-based Alert-Net network. They have proposed two-hybrid networks: Alert-Net-R and Alert-Net-X by combining Alert-Net with ResNet [85] and Xception [130], respectively. They further modify these two networks by removing a dropout layer, which results in two new networks: Alert-Net-RWD and Alert-Net-XWD.

Vogado *et al.* [35] have presented VGG-f [90]-based feature extraction followed by PCA-based feature reduction techniques to extract crucial features. Finally, they have employed an ensemble classifier to classify benign and malignant efficiently. Vogado *et al.* [4] have applied AlexNet [91], CaffNet [92], VGG-f [90] to extract efficient features. Then, they have used gain-ratio to select more important features.

Shahin *et al.* [79] have suggested transfer learning-based feature extraction scheme, where they have applied OverfeatNet [93], AlexNet [91], and VGGNet [90] for feature extraction. Then, they have used Chi-squared or PCA-based feature selection followed by SVM-based classification. In 2021, Das and Meher [7] have suggested a ShuffleNet-based ALL detection model, which yields promising performance by retaining advantages of channel shuffling, depthwise separable convolution, and group convolution. Genovese *et al.* [134] have recommended a VGG16-based ALL classification model in which an adaptive unsharpening technique is employed for image enhancement.

In 2021, Mondal *et al.* [135] have suggested an ensemble model by ensembling five popular transfer learning techniques: DenseNet, InceptionResNet-V2, VGG-16, and MobileNet. Though it achieves comparatively better performance than the above five transfer learning techniques, it is computationally expensive. To overcome this issue, in 2021, Das and Meher [2] have suggested a new hybrid ALL detection model by combining the advantages of ResNet18 and MobileNetV2. It gives promising performance and is faster than ensemble techniques since the second classifier (ResNet18) is executed while MobileNetV2 depicts relatively poor performance.

B. OTHER ADVANCEMENTS IN CNN

Recently, several other efficient, faster CNN models have been suggested, along with transfer learning models. You only look once (YOLO) [136], YOLOv2 [137], YOLOv3 [138], and YOLOv4 [139] are some popular advanced faster CNN models. YOLO is an effective CNN method that becomes computationally efficient by employing a CNN architecture to simultaneously perform localization and classification tasks. Hence, it yields faster object detection [136]. It applies a convolutional layer to predict the location of a bounding box. However, it is suffering from a localization error issue [137]. YOLOv2 is a modified version of YOLO that employs anchor boxes instead of the convolutional layer to mitigate localization error. Hence, it results in better object detection and classification [137]. YOLOv3 is an improved version of YOLO that applies a logistic regression-based prediction approach to perfectly detect bounding boxes [138]. Ai-Qudah and Suen [140] have employed YOLOv2 [137] to classify healthily and ALL efficiently. YOLOv2 [137] is an improvised version of YOLO [136] that boosts both precision and speed. They notice that YOLOv2 [137] with random resize outperforms YOLOv3 [138] and YOLOV2 [137] without random resize.

In 2020, Bochkovskiy *et al.* [139] have proposed the YOLOv4 model, in which cross-Stage-Partial-connections, weighted-Residual-Connections, cross mini-Batch Normalization, mish-activation, and self-adversarial-training is employed to boost the performance. In 2021, Khandekar *et al.* [141] have suggested the YOLOv4-based ALL classification model to classify healthy and ALL efficiently as it retains all the benefits of YOLOv4, as mentioned above.

In addition, several CNN-based advanced schemes are developed by various researchers for efficient disease diagnosis, particularly for cancer detection [40], [142]–[144]. Gehlot *et al.* [142] have suggested two-module deep learning ALL classification framework. In one module, compact CNN is employed that acts as the main classifier, whereas in another module, kernel SVM is applied that behaves as an auxiliary classifier. Duggal *et al.* [143] have presented an efficient CNN-based cancer detection system in which a stain deconvolutional (SD) layer is introduced to convert microscopic images to Optical Density (OD) space. It is also responsible for deconvolving these OD images by backpropagation learning to produce tissue-specific stain-absorption quantities as input to the next layer.

C. RECURRENT NEURAL NETWORK (RNN)

RNN is a deep learning technique that uses the current state's output to evaluate the next state's output. Hence, the effect of feedback in the network made it popular in the field of streaming data [27]. Bidirectional RNN [145], long short-term memory (LSTM) [146].

Bidirectional RNN is a modified version of RNN that can train the data both in positive and negative time directions [145]. LSTM [146] is an efficient RNN technique that can overcome the vanishing gradient issues. In LSTM, long-term information is stored in memory-cells, whereas conceptual information is learned to make the classification efficient. It uses a particular kind of memory block in place of nonlinear hidden units, unlike conventional RNN [146], [147]. In 2019, Shah *et al.* [148] suggested an efficient deep learning model by integrating the benefits of transfer learning (AlexNet) and RNN (LSTM).

D. AUTOENCODER

Autoencoder is a deep learning technique that transforms input to output with an optimum error. It maps a higher dimensional input into a lower-dimensional output [27], [57]. Usually, the input of the autoencoder is images or feature vectors. It comprises an encoder, decoder, and a loss function. Both encoder and decoder are neural networks. The encoder converts input (X) to output (Y) based on hidden layer size. The decoder is used to predict X from Y. Internally, an autoencoder consists of a hidden layer H, which describes a code employed for representing the input [149]. Its encoder is represented as:

$$F_e : X \rightarrow H \tag{8}$$

Hence,

$$H = F_e(X) \tag{9}$$

Similarly, the decoder is expressed as:

$$F_d : H \rightarrow Y \tag{10}$$

Thus,

$$Y = F_d(H) \tag{11}$$

where, F_e and F_d represent the encoder function and decoder function, respectively. Fig. 14 represents the general architecture of an autoencoder.

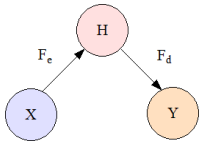

FIGURE 14. The architecture of an autoencoder.

If the learning of an autoencoder is simply designed to get $F_d(F_e(X)) = X$ everywhere, then it is not so useful. In contrast, it is designed for coping the input approximately, i.e., coping only input that resembles the training data. This model is designed to copy the particular aspects of input in a priority manner. Usually, an autoencoder learns crucial properties of data [149]. Hegde *et al.* [57] have employed autoencoder to classify WBCs into: monocyte, lymphocyte, basophil, eosinophil, neutrophil, and unhealthy WBC.

VII. PERFORMANCE MEASURES

The mathematical representation of various performance measures that have an essential role in comparative quantitative performance analysis is presented in Table 1. True positive (TP) presents the number of properly-identified ALL-affected-pixels. True Negative (TN) depicts accurately identified healthy-pixels. FN presents the number of inaccurately detected healthy-pixels. FP presents the number of falsely detected ALL-affected-pixels.

TABLE 1. Performance measures.

Performance Measures	Mathematical Representation
Specificity or True Negative Rate (TNR)	$\frac{TN}{(TN+FP)}$
Sensitivity or Recall or True Positive Rate (TPR)	$\frac{TP}{(TP+FN)}$
Precision	$\frac{TP}{(TP+FP)}$
Accuracy	$\frac{(TN+TP)}{(TN+TP+FN+FP)}$
F1 Score	$\frac{2(Precision*Recall)}{(Precision+Recall)}$
False Positive Rate (FPR)	$1 - specificity$

TABLE 2. ALL datasets.

Datasets	Description
ALLIDB1 [28]	It has 108 images that contain multiple leukocytes. Out of these 108 images, 59 are healthy, and 49 are ALL -affected images. Link- https://homes.di.unimi.it/scotti/all/
ALLIDB2 [28]	It has 130 healthy and 130 ALL affected images. Each image contains a single leukocyte. Link- https://homes.di.unimi.it/scotti/all/
Atlas	It contains 25 ALL, 40 AML, and 23 other types of images [126]. Link- http://www.hematologyatlas.com/principalpage.htm
BCCD	It consists of two sets of data. In first set, it contains 367 microscopic images (without argumentation). In another set, it contains 12444 images (with argumentation) [3]. Link- https://github.com/Shenggan/BCCD_Dataset
C-NMC	It contains 15000+ cancer cell images of B-Lineage ALL (B-ALL) along with healthy images. [150]. Link- https://competitions.codalab.org/competitions/20395

VIII. DATASET

Table 2 represents various publicly available standard datasets. Among these datasets, ALLIDB1 and ALLIDB2 datasets are two quite popular ALL datasets.

Among all these available datasets, ALLIDB1 and ALLIDB2 are the most popular standard datasets.

IX. TECHNICAL DISCUSSION

In this section, we demonstrate a comparative performance analysis of various deep and machine learning methods that are employed for the detection and classification of ALL.

Here, a comparative analysis is performed using the results as presented in their respective work. A comparative analysis of recent advancements in machine learning and deep learning-based ALL detection and classification is presented in Table 3.

Table 4 and Fig. 15 illustrate the segmentation performance using BCCD, whereas Table 5 and Fig. 16 represent the segmentation performance in ALL-IDB2 datasets. These tables and figures indicate the CNN-based segmentation model suggested by Banik *et al.* [3] yields superior performance in both the datasets with an accuracy of 99.42% and 98.61%, respectively. It yields good performance due to the fusion of features of the first and last convolution layers.

Table 6 and Fig. 17 represent machine learning-based ALL classification performance in ALL-IDB1 dataset. They indicate the ADBRF-based ALL classification approach suggested in [8] outperforms other machine learning approaches. The DOST-based feature-extraction before PCA-LDA-based feature-selection helps to extract more significant features, whereas ADBRF-based classification results in more efficient ALL classification. Hence, it achieves superior performance with the best sensitivity (100.00%) and best accuracy (99.66%). The SVM-based classification along with GLRLM-based feature extraction followed by PPCA-based feature selection recommended in [16] depicts the second-best accuracy (96.97%).

On the other hand, the ALL detection approaches proposed in [10] and [17] deliver similar accuracy performance

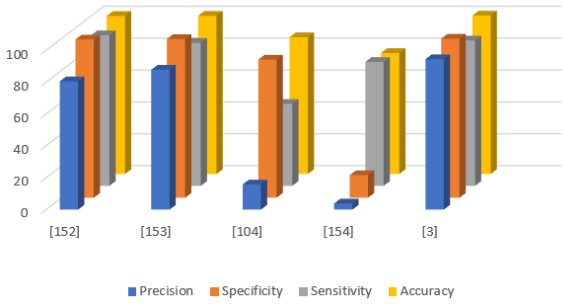

FIGURE 15. Graphical representation of segmentation performance using BCCD dataset.

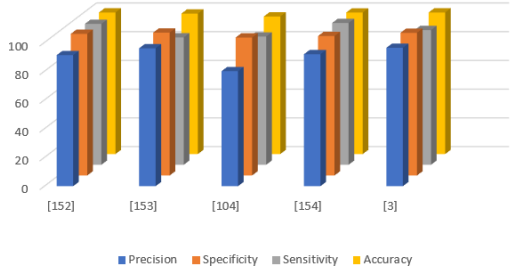

FIGURE 16. Graphical representation of segmentation performance using ALLIDB2 dataset.

(96.00%). The SVM-based ALL classification model recommended in [10] integrates benefits of color and shape features with GLRLM and GLCM-based texture features along with PCA-based feature selection that helps to achieve 93.06% specificity and 92.64% accuracy. The RF-based model suggested in [17] yields the best specificity (99.56%), the best accuracy(99.60%) and the best F1 Score (0.9973) among all machine learning-based ALL classification models. In contrast, it achieves poor sensitivity performance (86.50%) due to higher false negatives. The ensemble classifiers: E1 (ensemble of NaiveBayes, Decision tree, KNN, and SVM) and E2 (ensemble of SVM kernels: linear, polynomial, Gaussian radial-basis, quadratic, and multi-layer perceptron) suggested in [19] yield the best sensitivity (100%), whereas they give poor specificity, precision, and accuracy performances due to high false positives.

Table 7 and Fig. 18 illustrates deep learning-based ALL classification performance in the ALL-IDB1 dataset. It indicates hybrid ALL detection model proposed in [2] outperforms others with the best specificity, precision, accuracy, and F1 Score performances by combining the advantages of ResNet18 (residual learning and skip connection) and MobileNetV2 (linear bottleneck architecture, depthwise separable convolutions, and inverted residual). Moreover, MobileNetV2-SVM framework-based ALL classification scheme suggested by Das *et al.* [5] also yields excellent performance with the best accuracy of 99.39% and the best sensitivity of 100.00%. In that scheme, the benefits of the MobileNetV2-based feature extraction (linear bottleneck architecture, depthwise separable convolutions, and

TABLE 3. A comparative analysis of recent advancements in deep and machine learning-based detection and classification of ALL.

Refer-ence	Year	Segmen-tation	Features		Classifier	Dataset	Accuracy (%)
			Extarction	Reduction			
[34]	2017	Ostu's Thresholding	Shape, texture, and color	—	SVM	ALL-IDB1	89.80
[17]	2017	Watershed algorithm	GLCM	PPCA	RF	ALL-IDB1	96.00
[30]	2017	—	—	—	Ensemble transfer learning	—	88.50
[35]	2017	—	VGGNet	PCA	Ensemble	ALL-IDB1	100.00
[18]	2018	k-means	Texture, color, shape CD marker	—	k-means, SVM Deep learning	Private dataset	99.67
[29]	2018	k-means	Shape, color, size, texture	—	ANN, Decision Tree	ALL-IDB	99.52
[15]	2018	—	—	—	AlexNet	ALL-IDB2	96.06
[19]	2018	Watershed	Color, shape, LBP-based texture feature	—	Ensemble classifiers	ALL-IDB	89.81
[20]	2018	k-means clustering	Statistical, geometric, color textural feature.	—	kNN NB	Not revealed	92.80
[16]	2018	Watershed algorithm	GLRLM	—	SVM	ALL-IDB1	96.97
[4]	2018	—	Transfer learning	—	SVM	Hybrid dataset	99.20
[69]	2019	k-medoid	Shape, texture	—	ANN	ALL-IDB, Atlas, Online	98.60
[151]	2019	BSA	Color, texture, shape, statistical	Wavelet	Rough set	ALL-IDB	95.00
[73]	2019	FCM, Active Contour	Statistical	LDP	Deep CNN	ALL-IDB2	98.70
[57]	2019	Active contour thresholding	Shape, color texture	—	Auto encoder AlexNet	Private datset	99.00
[8]	2019	Triangle method of thresholding	DOST	PCA-LDA	ADBRF	ALL-IDB1	99.66
[79]	2019	—	Transfer learning	Chi-squared or PCA	SVM, Deep learning (WBCsNet)	ALL-IDB private datasets	96.10
[3]	2020	k-means	—	—	CNN	BCCD ALL-IDB2	99.42 98.61
[10]	2020	k-means	Color, shape texture (GLCM, GLRLM)	PCA	SVM	ALL-IDB1	96.00
[133]	2020	—	—	—	Deep Neural Network	Micro-array gene dataset	98.20
[84]	2020	DeepLabV3+	—	—	AlexNet	LISC	98.87
[126]	2020	—	—	—	Deep learning Transfer learning	Hybrid of 16 datasets	97.18
[140]	2020	—	—	—	YOLOv2	ALL-IDB1	98.72
[6]	2021	—	Transfer learning	—	Machine learning	ALL-IDB2	96.15
[134]	2021	—	—	—	VGG16	ALL-IDB2	96.84
[7]	2021	—	—	—	ShuffleNet	ALL-IDB1, ALL-IDB2	96.97 (ALL-IDB1) 96.97 (ALL-IDB2)
[141]	2021	—	—	—	YOLOv4	ALL-IDB1	— —
[2]	2021	—	—	—	Hybrid Transfer learning	ALL-IDB1, ALL-IDB2	99.39 (ALL-IDB1) 97.18 (ALL-IDB2)
[5]	2022	—	—	MobileNetV2	SVM	ALL-IDB1, ALL-IDB2	99.39 (ALL-IDB1) 98.21 (ALL-IDB2)

inverted residual) are combined with SVM-based classification (hyperplane location optimization) to give excellent performance. On the other hand, the ShuffleNet-based ALL detection model suggested in [7] yields the good performance by retaining advantages of channel shuffling, depthwise separable convolution, and group convolution.

TABLE 4. Segmentation performance using BCCD dataset.

Method	Precision (%)	Specificity (%)	Sensitivity (%)	Accuracy (%)
[152]	80.51	99.30	**94.51**	99.15
[153]	87.77	99.59	89.77	99.22
[104]	15.81	86.64	51.46	85.79
[154]	3.86	14.17	77.76	75.88
[3]	**94.38**	**99.78**	91.21	**99.42**

TABLE 5. Segmentation performance using ALLIDB2 dataset.

Method	Precision (%)	Specificity (%)	Sensitivity (%)	Accuracy (%)
[152]	91.24	98.62	98.09	98.59
[153]	96.00	**99.48**	88.70	97.81
[104]	80.09	96.05	89.27	95.80
[154]	91.89	97.10	**98.73**	98.54
[3]	**96.35**	99.33	93.80	**98.61**

TABLE 6. Machine learning-based classification performance in ALL-IDB1 dataset.

Method	Classifier	Specificity (%)	Sensitivity (%)	Precision (%)	Accuracy (%)	F1 Score
[19]	E1	54.24	**100.00**	64.47	75.00	0.7840
[19]	E2	81.36	**100.00**	81.67	89.81	0.8991
[34]	SVM	—	—	—	89.80	—
[17]	RF	**99.56**	86.50	**99.60**	96.00	0.9259
[10]	SVM	93.06	92.64	—	96.00	—
[16]	SVM	—	—	—	96.97	—
[8]	ADB-RF	99.12	**100.00**	99.46	**99.66**	**0.9973**

Table 8 depicts machine learning-based ALL classification performance with the ALL-IDB2 dataset. From the table, it is observed that Logistic Regression and SVM give the best sensitivity performance, whereas Random forest achieves the superior specificity, precision, and F1 Score performance among these machine learning schemes. Table 9 and Fig. 19 represents deep learning-based ALL classification performance with the ALL-IDB2 dataset. This table indicates most of the research works are based on transfer learning-based approaches due to their ability to achieve promising performance in small datasets. The MobileNetV2-SVM framework-based ALL classification scheme suggested by Das *et al.* [5] achieves the best accuracy (98.21%) and the best F1 Score (0.9828) performance. It delivers promising performance due to the combined benefits of the MobileNetV2-based feature extraction and SVM-based classification. We also observe the hybrid model suggested by Das and Meher [2] yields the second-best overall performance with 97.18% accuracy. It yields admirable performance due to the combined benefits of the MobileNetV2 and ResNet18. The ShuffleNet-based ALL detection model suggested in [7] achieves the second-best specificity, precision, and accuracy performance. On the other hand, Logistic Regression or SVM-based classification as suggested in [6] yields the best sensitivity (100%) due to the combined benefits of transfer learning-based feature extraction using modified ResNet model with machine learning-based classification. It delivers the third-best overall performance.

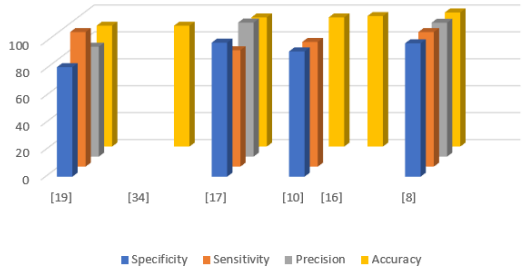

FIGURE 17. Graphical representation of machine learning-based classification performance in ALL-IDB1 dataset.

TABLE 7. Deep learning-based classification performance in ALL-IDB1 dataset.

Method	Classifier	Specificity (%)	Precision (%)	Sensitivity (%)	Accuracy (%)	F1 Score
[141]	YOLOv4	—	95.57	92.00	—	0.9375
[7]	Xception	93.89	90.00	62.00	80.61	0.7342
	NasNet-Mobile	96.66	94.62	76.00	85.15	0.8429
	VGG19	86.11	86.76	95.33	90.30	0.9084
	ResNet50	92.78	91.97	98.00	95.15	0.9489
	ShuffleNet	96.11	95.63	98.00	96.97	0.9680
[2]	AlexNet	89.35	89.55	98.64	93.64	0.9387
	VGG16	89.90	88.38	80.35	85.76	0.8417
	Google-Net	94.67	94.49	95.66	95.15	0.9507
	ResNet18	94.12	93.79	96.59	95.15	0.9517
	Mobile-NetV2	95.81	95.67	96.63	96.06	0.9615
	Hybrid	**99.47**	**99.33**	99.55	**99.39**	**0.9944**
[5]	VGG16	88.36	85.43	82.34	85.94	0.8384
	VGG16+ RF	91.36	89.76	85.79	89.62	0.8773
	VGG16+ SVM	95.00	92.03	87.33	91.48	0.8962
	Mobile-NetV2	97.00	95.72	96.19	95.68	0.9595
	Mobile-NetV2 +RF	98.00	97.33	96.19	96.29	0.9676
	Mobile-NetV2 +SVM	99.00	98.57	**100.00**	**99.39**	0.9926

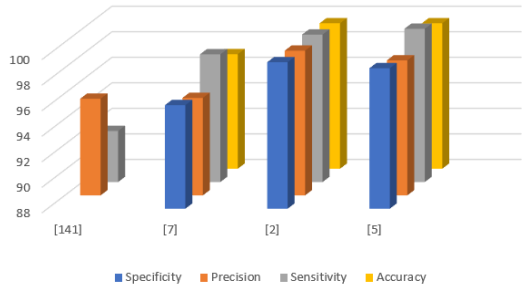

FIGURE 18. Graphical representation of deep learning-based classification performance in ALL-IDB1 dataset.

Goswami *et al.* [155] have suggested a transfer learning (InceptionV3)-based ALL detection scheme in which they have emphasized optimization of heterogeneity loss that helps the network for learning of subject-independent

TABLE 8. Machine learning-based classification performance with ALL-IDB2 dataset.

Method	Classifier	Specificity (%)	Precision (%)	Sensitivity (%)	Accuracy (%)	F1 Score
[6]	Random Forest	96.55	95.65	95.65	96.15	0.9565
	Logistic Regression	93.55	91.30	**100.00**	96.15	0.9545
	SVM	93.55	91.30	**100.00**	96.15	0.9545

TABLE 9. Deep learning-based classification performance with ALL-IDB2 dataset.

Method	Classifier	Specificity (%)	Precision (%)	Sensitivity (%)	Accuracy (%)	F1 Score
[7]	Xception	91.72	91.11	83.26	87.35	0.8701
	NasNet-Mobile	94.32	94.08	84.77	89.48	0.8918
	VGG19	78.76	80.93	88.45	83.59	0.8452
	ResNet50	94.82	94.82	92.90	93.85	0.9385
	ShuffleNet	96.90	96.95	96.46	96.67	0.9670
[134]	VGG16	96.15	—	97.53	96.84	—
[2]	AlexNet	88.21	89.77	94.87	91.54	0.9225
	VGG16	78.97	84.60	86.15	82.57	0.8537
	GoogleNet	86.67	88.26	96.41	91.54	0.9216
	ResNet18	93.34	93.82	93.34	93.34	0.9358
	MobileNetV2	93.84	95.48	91.80	92.82	0.9360
	Hybrid	**98.46**	**98.52**	95.90	97.18	0.9719
[5]	VGG16	82.00	83.04	88.13	85.22	0.8551
	VGG16+RF	86.05	86.42	87.53	86.92	0.8697
	VGG16+SVM	89.68	89.99	90.24	90.00	0.9011
	MobileNetV2	89.10	90.02	95.95	92.56	0.9289
	MobileNetV2+RF	92.63	93.58	96.95	94.87	0.9524
	MobileNetV2+SVM	97.37	97.61	**98.95**	**98.21**	**0.9828**

features. This proposed work is validated using the C-NMC dataset [150], which is the largest available ALL dataset. It achieves 95.26% of the weighted F1 score. Gupta and Gupta [156] have discussed some important challenging factors of the C-NMC dataset [150] that yields ALL detection tougher. The morphological similarity between ALL and healthy images, imbalanced dataset, and presence of inter-subject heterogeneity among images may enforce a system to learn subject-specific features rather than class-specific features [155]. Hence, these factors make the ALL classification more difficult.

Most of the research focuses on detecting ALL by classifying healthy or ALL-affected, whereas very few research works emphasize further classifying ALL to its subtypes (L1, L2, and L3). Table 10 represents AlexNet-based classification performance suggested in [15], which classifies WBCs into healthy and three ALL subtypes: L1, L2, and L3. It indicates L1 is the most accurately classified subtype among them. The suggested method achieves 96.06% overall accuracy.

TABLE 10. ALL sub-types classification performance using ALLIDB2 dataset.

	Normal	L1	L2	L3
Specificity (%)	99.00	**99.48**	98.40	99.26
Precision (%)	98.57	**99.60**	94.01	94.39
Sensitivity (%)	**100.00**	95.40	94.82	96.77
Accuracy (%)	98.11	**99.06**	93.33	93.75

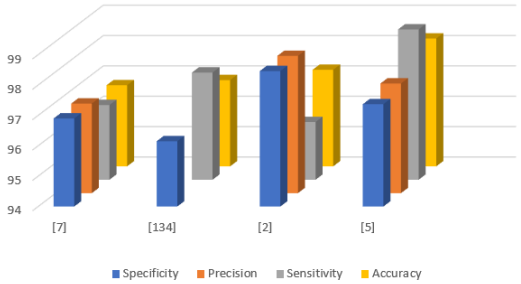

FIGURE 19. Graphical representation of deep learning-based classification performance with ALL-IDB2 dataset.

X. CRITICAL ANALYSIS

From this analysis, we observe that most of the signal and image processing-based methods are unable to deliver highly accurate segmentation due to the complex nature of cells, intensity inhomogeneities, and overlapping cells.

Unsupervised learning techniques are widely used in segmentation for detecting WBCs efficiently, as these techniques don't need labeled data for this purpose. However, in these techniques, selecting an appropriate number of clusters to yield excellent performance is still challenging. K-means is the most popular scheme for detecting desired WBCs due to its superior performance. However, in this scheme also, there is a challenge in selecting the appropriate cytoplasm and nucleus clusters as cluster index changes frequently even if the same algorithm is executed repeatedly. Hence, there is a need to select the desired clusters adaptively and carefully. On the other hand, transfer learning-based semantic segmentation (DeepLabV3+) achieves promising performance.

In most cases, we also observe that conventional machine learning-based classification approaches yield relatively poor performance since it requires proper segmentation before more accurate classification. However, the ADBRF-based ALL classification approach suggested in [8] achieves excellent performance with a 99.66% accuracy due to the combined benefits of RF as a base classifier with Adaboost learning. From this study, we also observed that unsupervised machine learning schemes are preferred over supervised ones for efficient WBC segmentation, whereas supervised machine learning schemes are preferred over unsupervised ones for more accurate classification. This occurs since, from the classification point of view, labeled data is publicly available (i.e., images with their class belongingness), whereas labeled segmentation data is not available.

In this review article, a brief analysis of recent advancements in deep and machine learning-based ALL detection

schemes is presented in a systematic manner. The conventional machine learning techniques require additional segmentation schemes for suppressing the presence of undesired cells and overlapping cells. In addition, the techniques require crucial hand-crafted geometrical, color, and texture features for more accurate classification. Hence, in these techniques, the overall classification performance relies on the performance of the preprocessing, segmentation, feature extraction, and classification stages. In contrast, a deep learning approach usually performs the segmentation, feature extraction, and classification tasks within a single neural network system. Unlike conventional machine learning approaches, it does not need an additional segmentation scheme. However, the traditional deep learning approach needs a large dataset for proper training to yield more efficient classification. Thus, traditional deep learning approaches are unable to achieve outstanding performance due to the unavailability of large labeled medical datasets. Recent developments in deep learning, particularly transfer learning approaches, help to solve this issue. In transfer learning approaches, a pretrained network trained in source-domain only finetuned in target-domain using small datasets; thus, it can also yield outstanding performance in the presence of small datasets. This is possible due to knowledge transfer from source to target domain.

Thus, transfer learning schemes are emerging as popular deep learning schemes for ALL detection because of their promising performance even in small datasets. Transfer learning-based method suggested in [35] achieves outstanding performance with 100% accuracy, whereas YOLOV2 based ALL classification method presented in [140] yields 98.72% accuracy. Among these transfer learning schemes, AlexNet, MobileNetV2, and ResNet are more popular due to their computational efficiency and classification performance. The MobileNetV2-SVM framework-based ALL classification scheme suggested by Das *et al.* [5] depicts promising performance by retaining benefits of MobileNetV2-based feature extraction and SVM-based classification. The hybrid transfer learning model suggested by Das and Meher [2] deliver excellent performance due to the combined advantages of ResNet18 and MobileNetV2.

Most of the researchers use two quite popular publicly available ALL datasets: ALLIDB1 and ALLIDB2 to detect and classify ALL. ALLIDB1 dataset is the most popular dataset for ALL detection, which is used in around 43.33% cases, whereas the ALLIDB2 dataset is used in around 40.00% cases. Among them, about 10% research work, both datasets are employed. From this review, we also observe that most of the research works only emphasize classifying healthy and ALL-affected. In only a few research work, ALL classification into its all subtypes are performed. This is one of the challenging future scopes in this field.

Holdout and k-Fold cross-validation are the two most popular schemes employed for effectively training and testing data. Holdout is the simplest scheme for evaluating a system (classifier) in which usually total data is split into training, testing, and validation subsets (sometimes training and testing subsets). For example, 70%, 20%, and 10% of data are applied for training, validation, and testing, respectively. However, in this scheme, a small portion of the total dataset images are used for testing, which is not so robust as the k-fold cross-validation scheme. Hence, it is recommended to demonstrate a comparative performance analysis using cross-validation. In k-Fold cross-validation, the dataset is divided into k groups in such a manner that each group contains the approximately same number of images with images from each class is also present. Then, in the first fold, the first group images are used for testing, whereas the remaining images are used for training. Similarly, in the second fold, the second group images are used for testing, whereas the remaining images are used for training. This will continue for all the k-folds. Finally, the average performance among these k-folds is compared for performance analysis. Thus, the cross-validation performance is more reliable and more robust than hold-out methods as in cross-validation approaches; each image is once used for testing. Usually, the performance comparison is done using 5-Fold or 10-Fold cross-validations.

XI. CHALLENGING ISSUES

An ALL detection and classification system may face the following challenging issues.

- Traditional deep learning approaches are unable to achieve outstanding performance due to the unavailability of large labeled datasets.
- The presence of overlapping cells, weak edges, noise, and intensity inhomogeneity result the segmentation and classification more challenging.
- Illumination variation may yield non-uniform color distribution for cytoplasm and nucleus regions. Thus, proper discrimination in these regions becomes more difficult.
- The shape, size, texture, and morphological structure of the nucleus and cytoplasm vary for different subtypes of WBCs (Basophil, Neutrophil, Eosinophil, monocyte, or lymphocyte). Hence, it makes the classification of benign and malignant more challenging.
- Classification of ALL into its subtypes: L1, L2, and L3 become a tough job due to standard-labeled datasets' unavailability.

XII. FUTURE SCOPES

As discussed above, many efficient machine learning and deep learning-based ALL classification systems have been suggested by various researchers. However, there are still scopes for further research to improve the performance and make the ALL diagnosis more accurate and robust, as given below.

- A new hybrid dataset can be created by combining images of various illuminations, resolutions, and size, which gives an opportunity to build more robust systems for ALL detection and classification.

- Segmentation performance can be boost by hybridizing an efficient active contour/ level set method with the marker-based watershed algorithm or hybridizing the level set method with deep learning techniques.
- Efficient deep learning (particularly transfer learning)-based method may yield more accurate segmentation.
  Research can be carried out to develop a more efficient deep learning (particularly transfer learning)-based ALL segmentation system.
  More advanced deep learning or transfer learning-based systems can be designed by modifying the existing efficient models to make the system more accurate and faster as well. For example, the softmax layer or fully-connected classification layer can be replaced by more efficient classification layers to make the optimization easier and minimize the co-adaption among parameters in the classification layer. The number of connections can be minimized by selecting more significant and desired connections to improve the inter-class angles. Hence, the system can be more efficient and faster.
- Classification performance can be improved by suggesting more efficient and robust machine learning, deep learning, or transfer learning methods.
  Research can be carried out to develop a more efficient ALL detection system by integrating the benefits of transfer learning-based feature extraction with machine learning-based classification.
  More advanced deep learning or transfer learning-based systems can be designed by modifying the existing efficient models to make the system more accurate and faster as well. For example, the softmax layer or fully-connected classification layer can be replaced by more efficient classification layers in which only significant and desired connections are employed to improve the angle between the features and co-adaption among features.
- The performance can be further enhanced by employing an ensemble or hybrid of the above classifiers.
  The ALL classification performance can be improved by employing an efficient ensemble transfer learning classifier that combines the benefits of all the transfer learning schemes used in this classifier. Hence, it enhances the diversity ability of feature learning, resulting in the extraction of more significant features. In addition, the combined benefits also improve the overall classification performances.
  The ALL classification performance can be improved by suggesting more efficient hybrid systems like the MobileNetV2-ResNet18 hybrid classifier discussed in this article. More efficient transfer learning schemes can be hybridized to further improve the ALL classification performance and also make the system faster, keeping the benefits of the hybridizing models. More importantly, research can be carried out to develop more efficient ensemble transfer learning classifiers or to develop more efficient hybrid transfer learning classifiers since transfer learning schemes achieves promising performance with small datasets also.
- Further research can be carried out to efficiently classify benign and malignant (ALL) as well as classify ALL into its subtypes: L1, L2, and L3, which results in more accurate disease diagnosis.

XIII. CONCLUSION

This article presents a brief analysis of recent advancements in deep and machine learning-based detection and classification of ALL. We have analyzed various existing methods of segmentation, feature extraction, and classification, which are employed to detect ALL efficiently. From this review, we also observed that among classical machine learning schemes, unsupervised schemes are preferred for segmentation tasks, whereas supervised schemes are preferred for classification tasks. However, Deep learning, particularly transfer learning, has emerged as a preferred approach for automatic and more robust detection and classification of ALL since it yields excellent performance even in small datasets. From this study, we have also observed that the MobileNetV2-ResNet18 architecture yields the best ALL detection performance in ALLIDB1 dataset due to the combined benefits of both schemes. In the ALLIDB2 dataset, MobileNetV2-SVM depicts admirable classification performance by integrating the pros of both approaches. Furthermore, we have discussed the challenging issues and future scope in this research field. We hope this article will help researchers to analyze recent advancements in ALL detection and will inspire researchers to do further research.

REFERENCES

[1] P. K. Das, S. Meher, R. Panda, and A. Abraham, "An efficient blood-cell segmentation for the detection of hematological disorders," *IEEE Trans. Cybern.*, early access, Mar. 18, 2021, doi: 10.1109/TCYB.2021.3062152.

[2] P. K. Das and S. Meher, "An efficient deep convolutional neural network based detection and classification of acute lymphoblastic leukemia," *Expert Syst. Appl.*, vol. 183, Nov. 2021, Art. no. 115311.

[3] P. P. Banik, R. Saha, and K.-D. Kim, "An automatic nucleus segmentation and CNN model based classification method of white blood cell," *Expert Syst. Appl.*, vol. 149, Jul. 2020, Art. no. 113211.

[4] L. H. Vogado, R. M. S. Veras, F. H. D. Araujo, R. R. V. Silva, and K. R. T. Aires, "Leukemia diagnosis in blood slides using transfer learning in CNNs and SVM for classification," *Eng. Appl. Artif. Intell.*, vol. 72, pp. 415–422, Jun. 2018.

[5] P. K. Das, B. Nayak, and S. Meher, "A lightweight deep learning system for automatic detection of blood cancer," *Measurement*, vol. 191, Mar. 2022, Art. no. 110762.

[6] P. K. Das, A. Pradhan, and S. Meher, "Detection of acute lymphoblastic leukemia using machine learning techniques," in *Machine Learning, Deep Learning and Computational Intelligence for Wireless Communication*. Singapore: Springer, 2021, pp. 425–437.

[7] P. K. Das and S. Meher, "Transfer learning-based automatic detection of acute lymphocytic leukemia," in *Proc. Nat. Conf. Commun. (NCC)*, Jul. 2021, pp. 1–6.

[8] S. Mishra, B. Majhi, and P. K. Sa, "Texture feature based classification on microscopic blood smear for acute lymphoblastic leukemia detection," *Biomed. Signal Process. Control*, vol. 47, pp. 303–311, Jan. 2019.

[9] P. K. Das, S. Meher, R. Panda, and A. Abraham, "A review of automated methods for the detection of sickle cell disease," *IEEE Rev. Biomed. Eng.*, vol. 13, pp. 309–324, 2020.

[10] P. K. Das, P. Jadoun, and S. Meher, "Detection and classification of acute lymphocytic leukemia," in *Proc. IEEE-HYDCON*, Sep. 2020, pp. 1–5.
[11] N. Patel and A. Mishra, "Automated leukaemia detection using microscopic images," *Proc. Comput. Sci.*, vol. 58, pp. 635–642, Jan. 2015.
[12] J. M. Bennett, D. Catovsky, M.-T. Daniel, G. Flandrin, D. A. G. Galton, H. R. Gralnick, and C. Sultan, "Proposals for the classification of the acute leukaemias French-American-British (FAB) co-operative group," *Brit. J. Haematol.*, vol. 33, no. 4, pp. 451–458, Aug. 1976.
[13] T. Terwilliger and M. Abdul-Hay, "Acute lymphoblastic leukemia: A comprehensive review and 2017 update," *Blood Cancer J.*, vol. 7, no. 6, p. e577, Jun. 2017.
[14] K. AL-Dulaimi, J. Banks, K. Nugyen, A. Al-Sabaawi, I. Tomeo-Reyes, and V. Chandran, "Segmentation of white blood cell, nucleus and cytoplasm in digital haematology microscope images: A review–challenges, current and future potential techniques," *IEEE Rev. Biomed. Eng.*, vol. 14, pp. 290–306, 2021.
[15] S. Shafique and S. Tehsin, "Acute lymphoblastic leukemia detection and classification of its subtypes using pretrained deep convolutional neural networks," *Technol. Cancer Res. Treatment*, vol. 17, Sep. 2018, Art. no. 1533033818802789.
[16] S. Mishra, B. Majhi, and P. K. Sa, "GLRLM-based feature extraction for acute lymphoblastic leukemia (ALL) detection," in *Recent Findings in Intelligent Computing Techniques*. Singapore: Springer, 2018, pp. 399–407.
[17] S. Mishra, B. Majhi, P. K. Sa, and L. Sharma, "Gray level co-occurrence matrix and random forest based acute lymphoblastic leukemia detection," *Biomed. Signal Process. Control*, vol. 33, pp. 272–280, Mar. 2017.
[18] J. Laosai and K. Chamnongthai, "Classification of acute leukemia using medical-knowledge-based morphology and CD marker," *Biomed. Signal Process. Control*, vol. 44, pp. 127–137, Jul. 2018.
[19] Z. Moshavash, H. Danyali, and M. S. Helfroush, "An automatic and robust decision support system for accurate acute leukemia diagnosis from blood microscopic images," *J. Digit. Imag.*, vol. 31, no. 5, pp. 702–717, Oct. 2018.
[20] S. Kumar, S. Mishra, and P. Asthana, "Automated detection of acute leukemia using K-mean clustering algorithm," in *Advances in Computer and Computational Sciences*. Singapore: Springer, 2018, pp. 655–670.
[21] T. Ojala, M. Pietikäinen, and T. Mäenpää, "Multiresolution gray-scale and rotation invariant texture classification with local binary patterns," *IEEE Trans. Pattern Anal. Mach. Intell.*, vol. 24, no. 7, pp. 971–987, Jul. 2002.
[22] T. Jabid, M. H. Kabir, and O. Chae, "Local directional pattern (LDP) for face recognition," in *Proc. Dig. Tech. Papers Int. Conf. Consum. Electron. (ICCE)*, Jan. 2010, pp. 329–330.
[23] S. Drabycz, R. G. Stockwell, and J. R. Mitchell, "Image texture characterization using the discrete orthonormal S-transform," *J. Digit. Imag.*, vol. 22, no. 6, p. 696, 2009.
[24] R. M. Haralick, K. Shanmugam, and I. Dinstein, "Textural features for image classification," *IEEE Trans. Syst., Man, Cybern.*, vol. SMC-3, no. 6, pp. 610–621, Nov. 1973.
[25] X. Tang, "Texture information in run-length matrices," *IEEE Trans. Image Process.*, vol. 7, no. 11, pp. 1602–1609, Nov. 1998.
[26] E. H. Houssein, M. M. Emam, A. A. Ali, and P. N. Suganthan, "Deep and machine learning techniques for medical imaging-based breast cancer: A comprehensive review," *Expert Syst. Appl.*, vol. 167, Apr. 2021, Art. no. 114161.
[27] M. Mahmud, M. S. Kaiser, A. Hussain, and S. Vassanelli, "Applications of deep learning and reinforcement learning to biological data," *IEEE Trans. Neural Netw. Learn. Syst.*, vol. 29, no. 6, pp. 2063–2079, Jun. 2018.
[28] R. D. Labati, V. Piuri, and F. Scotti, "All-IDB: The acute lymphoblastic leukemia image database for image processing," in *Proc. 18th IEEE Int. Conf. Image Process.*, Sep. 2011, pp. 2045–2048.
[29] A. S. Negm, O. A. Hassan, and A. H. Kandil, "A decision support system for acute leukaemia classification based on digital microscopic images," *Alexandria Eng. J.*, vol. 57, no. 4, pp. 2319–2332, Dec. 2018.
[30] W. Yu, J. Chang, C. Yang, L. Zhang, H. Shen, Y. Xia, and J. Sha, "Automatic classification of leukocytes using deep neural network," in *Proc. IEEE 12th Int. Conf. ASIC (ASICON)*, Oct. 2017, pp. 1041–1044.
[31] S. Mandal, V. Daivajna, and R. V., "Machine learning based system for automatic detection of leukemia cancer cell," in *Proc. IEEE 16th India Council Int. Conf. (INDICON)*, Dec. 2019, pp. 1–4.
[32] K. G. Dhal, J. Gálvez, S. Ray, A. Das, and S. Das, "Acute lymphoblastic leukemia image segmentation driven by stochastic fractal search," *Multimedia Tools Appl.*, vol. 79, pp. 1–29, May 2020.
[33] M. MoradiAmin, A. Memari, N. Samadzadehaghdam, S. Kermani, and A. Talebi, "Computer aided detection and classification of acute lymphoblastic leukemia cell subtypes based on microscopic image analysis," *Microsc. Res. Technique*, vol. 79, no. 10, pp. 908–916, Oct. 2016.
[34] J. Rawat, A. Singh, H. S. Bhadauria, J. Virmani, and J. S. Devgun, "Classification of acute lymphoblastic leukaemia using hybrid hierarchical classifiers," *Multimedia Tools Appl.*, vol. 76, no. 18, pp. 19057–19085, Sep. 2017.
[35] L. H. S. Vogado, R. D. M. S. Veras, A. R. Andrade, F. H. D. de Araujo, R. R. V. Silva, and K. R. T. Aires, "Diagnosing leukemia in blood smear images using an ensemble of classifiers and pre-trained convolutional neural networks," in *Proc. 30th SIBGRAPI Conf. Graph., Patterns Images (SIBGRAPI)*, Oct. 2017, pp. 367–373.
[36] R. G. Bagasjvara, I. Candradewi, S. Hartati, and A. Harjoko, "Automated detection and classification techniques of acute leukemia using image processing: A review," in *Proc. 2nd Int. Conf. Sci. Technology-Computer (ICST)*, Oct. 2016, pp. 35–43.
[37] A. Parthvi, K. Rawal, and D. K. Choubey, "A comparative study using machine learning and data mining approach for leukemia," in *Proc. Int. Conf. Commun. Signal Process. (ICCSP)*, Jul. 2020, pp. 0672–0677.
[38] K. K. Anilkumar, V. J. Manoj, and T. M. Sagi, "A survey on image segmentation of blood and bone marrow smear images with emphasis to automated detection of leukemia," *Biocybernetics Biomed. Eng.*, vol. 40, no. 4, pp. 1406–1420, Oct. 2020.
[39] A. Anghel, M. Stanisavljevic, S. Andani, N. Papandreou, J. H. Rüschoff, P. Wild, M. Gabrani, and H. Pozidis, "A high-performance system for robust stain normalization of whole-slide images in histopathology," *Frontiers Med.*, vol. 6, p. 193, Sep. 2019.
[40] S. Gehlot and A. Gupta, "Self-supervision based dual-transformation learning for stain normalization, classification andsegmentation," in *Proc. Int. Workshop Mach. Learn. Med. Imag.* Cham, Switzerland: Springer, 2021, pp. 477–486.
[41] I. Yoon, S. Kim, D. Kim, M. H. Hayes, and J. Paik, "Adaptive defogging with color correction in the HSV color space for consumer surveillance system," *IEEE Trans. Consum. Electron.*, vol. 58, no. 1, pp. 111–116, Feb. 2012.
[42] G.-H. Park, H.-H. Cho, and M.-R. Choi, "A contrast enhancement method using dynamic range separate histogram equalization," *IEEE Trans. Consum. Electron.*, vol. 54, no. 4, pp. 1981–1987, Nov. 2018.
[43] X. Jingbo, L. Bo, L. Haijun, and L. Jianxin, "A new method for realizing log filter in image edge detection," in *Proc. 6th Int. Forum Strategic Technol.*, vol. 2, Aug. 2011, pp. 733–737.
[44] C. Lian, M. Liu, J. Zhang, and D. Shen, "Hierarchical fully convolutional network for joint atrophy localization and Alzheimer's disease diagnosis using structural MRI," *IEEE Trans. Pattern Anal. Mach. Intell.*, vol. 42, no. 4, pp. 880–893, Apr. 2020.
[45] J. Rawat, A. Singh, B. Hs, J. Virmani, and J. S. Devgun, "Computer assisted classification framework for prediction of acute lymphoblastic and acute myeloblastic leukemia," *Biocybernetics Biomed. Eng.*, vol. 37, no. 4, pp. 637–654, 2017.
[46] J. Zhao, M. Zhang, Z. Zhou, J. Chu, and F. Cao, "Automatic detection and classification of leukocytes using convolutional neural networks," *Med. Biol. Eng. Comput.*, vol. 55, no. 8, pp. 1287–1301, Aug. 2017.
[47] D. Umamaheswari and S. Geetha, "Segmentation and classification of acute lymphoblastic leukemia cells tooled with digital image processing and ML techniques," in *Proc. 2nd Int. Conf. Intell. Comput. Control Syst. (ICICCS)*, Jun. 2018, pp. 1336–1341.
[48] G. W. Zack, W. E. Rogers, and S. A. Latt, "Automatic measurement of sister chromatid exchange frequency," *J. Histochem. Cytochem.*, vol. 25, no. 7, pp. 741–753, 1977.
[49] L. B. Dorini, R. Minetto, and N. J. Leite, "White blood cell segmentation using morphological operators and scale-space analysis," in *Proc. 20th Brazilian Symp. Comput. Graph. Image Process. (SIBGRAPI)*, Oct. 2007, pp. 294–304.
[50] L. B. Dorini, R. Minetto, and N. J. Leite, "Semiautomatic white blood cell segmentation based on multiscale analysis," *IEEE J. Biomed. Health Informat.*, vol. 17, no. 1, pp. 250–256, Jan. 2012.
[51] M. A. Fadhel, A. J. Humaidi, and S. R. Oleiwi, "Image processing-based diagnosis of sickle cell anemia in erythrocytes," in *Proc. Annu. Conf. New Trends Inf. Commun. Technol. Appl. (NTICT)*, Mar. 2017, pp. 203–207.
[52] Anita and A. Yadav, "An intelligent model for the detection of white blood cells using artificial intelligence," *Comput. Methods Programs Biomed.*, vol. 199, Feb. 2021, Art. no. 105893.

[53] M. Kass, A. Witkin, and D. Terzopoulos, "Snakes: Active contour models," *Int. J. Comput. Vis.*, vol. 1, no. 4, pp. 321–331, 1988.

[54] S. Eom, S. Kim, V. Shin, and B. Ahn, "Leukocyte segmentation in blood smear images using region-based active contours," in *Proc. Int. Conf. Adv. Concepts Intell. Vis. Syst.* Berlin, Germany: Springer, 2006, pp. 867–876.

[55] C. Li, C. Xu, C. Gui, and M. D. Fox, "Distance regularized level set evolution and its application to image segmentation," *IEEE Trans. Image Process.*, vol. 19, no. 12, pp. 3243–3254, Dec. 2010.

[56] A. Khadidos, V. Sanchez, and C.-T. Li, "Weighted level set evolution based on local edge features for medical image segmentation," *IEEE Trans. Image Process.*, vol. 26, no. 4, pp. 1979–1991, Apr. 2017.

[57] R. B. Hegde, K. Prasad, H. Hebbar, and B. M. K. Singh, "Comparison of traditional image processing and deep learning approaches for classification of white blood cells in peripheral blood smear images," *Biocybernetics Biomed. Eng.*, vol. 39, no. 2, pp. 382–392, Apr. 2019.

[58] C. Cortes and V. Vapnik, "Support-vector networks," *Mach. Learn.*, vol. 20, pp. 273–297, Apr. 1995.

[59] J. J. Hopfield, "Artificial neural networks," *IEEE Circuits Devices Mag.*, vol. DM-4, no. 5, pp. 3–10, Sep. 1988.

[60] M. H. Hassoun, *Fundamentals of Artificial Neural Networks*. Cambridge, MA, USA: MIT Press, 1995.

[61] M. Pal, "Random forest classifier for remote sensing classification," *Int. J. Remote Sens.*, vol. 26, no. 1, pp. 217–222, 2005.

[62] E. Abdulhay, M. A. Mohammed, D. A. Ibrahim, N. Arunkumar, and V. Venkatraman, "Computer aided solution for automatic segmenting and measurements of blood leucocytes using static microscope images," *J. Med. Syst.*, vol. 42, no. 4, p. 58, 2018.

[63] S. Mohapatra, D. Patra, S. Kumar, and S. Satpathy, "Lymphocyte image segmentation using functional link neural architecture for acute leukemia detection," *Biomed. Eng. Lett.*, vol. 2, no. 2, pp. 100–110, Jun. 2012.

[64] J. C. Patra, R. N. Pal, B. N. Chatterji, and G. Panda, "Identification of nonlinear dynamic systems using functional link artificial neural networks," *IEEE Trans. Syst., Man, Cybern. B, Cybern.*, vol. 29, no. 2, pp. 254–262, Apr. 1999.

[65] J. C. Patra, G. Panda, and R. Baliarsingh, "Artificial neural network-based nonlinearity estimation of pressure sensors," *IEEE Trans. Instrum. Meas.*, vol. 43, no. 6, pp. 874–881, Dec. 1994.

[66] J. A. Hartigan and M. A. Wong, "Algorithm AS 136: A K-means clustering algorithm," *Appl. Statist.*, vol. 28, no. 1, pp. 100–108, Jan. 1979.

[67] A. Likas, N. Vlassis, and J. J. Verbeek, "The global K-means clustering algorithm," *Pattern Recognit.*, vol. 36, no. 2, pp. 451–461, Feb. 2003.

[68] J. C. Bezdek, W. Full, and R. Ehrlich, "FCM: The fuzzy C-means clustering algorithm," *Comput. Geosci.*, vol. 10, nos. 2–3, pp. 191–203, 1984.

[69] V. Acharya and P. Kumar, "Detection of acute lymphoblastic leukemia using image segmentation and data mining algorithms," *Med. Biol. Eng. Comput.*, vol. 57, no. 8, pp. 1783–1811, Aug. 2019.

[70] S. Mohapatra, D. Patra, and S. Satpathi, "Image analysis of blood microscopic images for acute leukemia detection," in *Proc. Int. Conf. Ind. Electron., Control Robot.*, Dec. 2010, pp. 215–219.

[71] K.-S. Chuang, H.-L. Tzeng, S. Chen, J. Wu, and T.-J. Chen, "Fuzzy c-means clustering with spatial information for image segmentation," *Comput. Med. Imag. Graph.*, vol. 30, pp. 9–15, Jan. 2006.

[72] S. Mohapatra, D. Patra, and K. Kumar, "Unsupervised leukocyte image segmentation using rough fuzzy clustering," *ISRN Artif. Intell.*, vol. 2012, pp. 1–12, Mar. 2012.

[73] K. K. Jha and H. S. Dutta, "Mutual information based hybrid model and deep learning for acute lymphocytic leukemia detection in single cell blood smear images," *Comput. Methods Programs Biomed.*, vol. 179, Oct. 2019, Art. no. 104987.

[74] Q. Wang, S. Bi, M. Sun, Y. Wang, D. Wang, and S. Yang, "Deep learning approach to peripheral leukocyte recognition," *PLoS ONE*, vol. 14, no. 6, Jun. 2019, Art. no. e0218808.

[75] W. Liu, D. Anguelov, D. Erhan, C. Szegedy, S. Reed, C.-Y. Fu, and A. C. Berg, "SSD: Single shot multibox detector," in *Proc. Eur. Conf. Comput. Vis.* Cham, Switzerland: Springer, 2016, pp. 21–37.

[76] J. Redmon and A. Farhadi, "YOLOv3: An incremental improvement," 2018, *arXiv:1804.02767*.

[77] S. Mandal, V. Daivajna, S. Kalsangra, V. Rajagopalan, and A. Kuchlous, "Computer aided system for automatic detection and marking instance of nuclei," in *Proc. IEEE Int. Conf. Electr., Comput. Commun. Technol. (ICECCT)*, Feb. 2019, pp. 1–6.

[78] O. Ronneberger, P. Fischer, and T. Brox, "U-Net: Convolutional networks for biomedical image segmentation," in *Proc. Int. Conf. Med. Image Comput.-Assist. Intervent*. Cham, Switzerland: Springer, 2015, pp. 234–241.

[79] A. I. Shahin, Y. Guo, K. M. Amin, and A. A. Sharawi, "White blood cells identification system based on convolutional deep neural learning networks," *Comput. Methods Programs Biomed.*, vol. 168, pp. 69–80, Jan. 2019.

[80] R. Duggal, A. Gupta, R. Gupta, M. Wadhwa, and C. Ahuja, "Overlapping cell nuclei segmentation in microscopic images using deep belief networks," in *Proc. 10th Indian Conf. Comput. Vis., Graph. Image Process. (ICVGIP)*, 2016, pp. 1–8.

[81] N. Kumar, R. Verma, S. Sharma, S. Bhargava, A. Vahadane, and A. Sethi, "A dataset and a technique for generalized nuclear segmentation for computational pathology," *IEEE Trans. Med. Imag.*, vol. 36, no. 7, pp. 1550–1560, Jul. 2017.

[82] A. Gupta, P. Mallick, O. Sharma, R. Gupta, and R. Duggal, "PCSeg: Color model driven probabilistic multiphase level set based tool for plasma cell segmentation in multiple myeloma," *PLoS ONE*, vol. 13, no. 12, Dec. 2018, Art. no. e0207908.

[83] S. Gehlot, A. Gupta, and R. Gupta, "EDNFC-Net: Convolutional neural network with nested feature concatenation for nuclei-instance segmentation," in *Proc. IEEE Int. Conf. Acoust., Speech Signal Process. (ICASSP)*, May 2020, pp. 1389–1393.

[84] M. R. Reena and P. M. Ameer, "Localization and recognition of leukocytes in peripheral blood: A deep learning approach," *Comput. Biol. Med.*, vol. 126, Nov. 2020, Art. no. 104034.

[85] K. He, X. Zhang, S. Ren, and J. Sun, "Deep residual learning for image recognition," in *Proc. IEEE Conf. Comput. Vis. Pattern Recognit.*, Jun. 2016, pp. 770–778.

[86] S. Wold, K. Esbensen, and P. Geladi, "Principal component analysis," *Chemometrics Intell. Lab. Syst.*, vol. 2, nos. 1–3, pp. 37–52, 1987.

[87] M. E. Tipping and C. M. Bishop, "Probabilistic principal component analysis," *J. Roy. Statist. Soc. B*, vol. 61, no. 3, pp. 611–622, 1999.

[88] H. Yu and J. Yang, "A direct LDA algorithm for high-dimensional data—With application to face recognition," *Pattern Recognit.*, vol. 34, no. 10, pp. 2067–2070, Oct. 2001.

[89] M.-C. Su, C.-Y. Cheng, and P.-C. Wang, "A neural-network-based approach to white blood cell classification," *Sci. World J.*, vol. 2014, pp. 1–9, Jan. 2014.

[90] K. Simonyan and A. Zisserman, "Very deep convolutional networks for large-scale image recognition," 2014, *arXiv:1409.1556*.

[91] A. Krizhevsky, I. Sutskever, and G. E. Hinton, "ImageNet classification with deep convolutional neural networks," in *Proc. Adv. Neural Inf. Process. Syst.*, 2012, pp. 1097–1105.

[92] Y. Jia, E. Shelhamer, J. Donahue, S. Karayev, J. Long, R. Girshick, S. Guadarrama, and T. Darrell, "Caffe: Convolutional architecture for fast feature embedding," in *Proc. 22nd ACM Int. Conf. Multimedia*, 2014, pp. 675–678.

[93] P. Sermanet, D. Eigen, X. Zhang, M. Mathieu, R. Fergus, and Y. LeCun, "OverFeat: Integrated recognition, localization and detection using convolutional networks," 2013, *arXiv:1312.6229*.

[94] T. Cover and P. Hart, "Nearest neighbor pattern classification," *IEEE Trans. Inf. Theory*, vol. IT-13, no. 1, pp. 21–27, Jan. 1967.

[95] I. Rish, "An empirical study of the naive Bayes classifier," in *Proc. IJCAI Workshop Empirical Methods Artif. Intell.*, vol. 3, no. 22, 2001, pp. 41–46.

[96] D. W. Ruck, S. K. Rogers, M. Kabrisky, M. E. Oxley, and B. W. Suter, "The multilayer perceptron as an approximation to a Bayes optimal discriminant function," *IEEE Trans. Neural Netw.*, vol. 1, no. 4, pp. 296–298, Dec. 1990.

[97] J. R. Quinlan, "Induction of decision trees," *Mach. Learn.*, vol. 1, no. 1, pp. 81–106, 1986.

[98] L. Breiman, "Random forests," *Mach. Learn.*, vol. 45, no. 1, pp. 5–32, 2001.

[99] S. B. Kotsiantis, I. Zaharakis, and P. Pintelas, "Supervised machine learning: A review of classification techniques," *Emerg. Artif. Intell. Appl. Comput. Eng.*, vol. 160, pp. 3–24, Oct. 2007.

[100] J. Cervantes, F. Garcia-Lamont, L. Rodríguez-Mazahua, and A. Lopez, "A comprehensive survey on support vector machine classification: Applications, challenges and trends," *Neurocomputing*, vol. 408, pp. 189–215, Sep. 2020.

[101] Y. Zhang, G. Cao, B. Wang, and X. Li, "A novel ensemble method for K-nearest neighbor," *Pattern Recognit.*, vol. 85, pp. 13–25, Jan. 2019.

[102] H. T. Madhloom, S. A. Kareem, and H. Ariffin, "A robust feature extraction and selection method for the recognition of lymphocytes versus acute lymphoblastic leukemia," in *Proc. Int. Conf. Adv. Comput. Sci. Appl. Technol. (ACSAT)*, Nov. 2012, pp. 330–335.
[103] D. M. U. Sabino, L. da Fontoura Costa, E. Gil Rizzatti, and M. Antonio Zago, "A texture approach to leukocyte recognition," *Real-Time Imag.*, vol. 10, no. 4, pp. 205–216, Aug. 2004.
[104] S. Nazlibilek, D. Karacor, T. Ercan, M. H. Sazli, O. Kalender, and Y. Ege, "Automatic segmentation, counting, size determination and classification of white blood cells," *Measurement*, vol. 55, no. 3, pp. 58–65, 2014.
[105] S. C. Neoh, W. Srisukkham, L. Zhang, S. Todryk, B. Greystoke, C. P. Lim, M. A. Hossain, and N. Aslam, "An intelligent decision support system for leukaemia diagnosis using microscopic blood images," *Sci. Rep.*, vol. 5, p. 14938, Oct. 2015.
[106] S. K. Murthy, "Automatic construction of decision trees from data: A multi-disciplinary survey," *Data Mining Knowl. Discovery*, vol. 2, no. 4, pp. 345–389, Dec. 1998.
[107] S. R. Safavian and D. Landgrebe, "A survey of decision tree classifier methodology," *IEEE Trans. Syst., Man, Cybern.*, vol. 21, no. 3, pp. 660–674, May/Jun. 1991.
[108] P. E. Hart, D. G. Stork, and R. O. Duda, *Pattern Classification*. Hoboken, NJ, USA: Wiley, 2006.
[109] T.-S. Lim, W.-Y. Loh, and Y.-S. Shih, "A comparison of prediction accuracy, complexity, and training time of thirty-three old and new classification algorithms," *Mach. Learn.*, vol. 40, no. 3, pp. 203–228, 2000.
[110] R. K. Amin and Y. Sibaroni, "Implementation of decision tree using C4. 5 algorithm in decision making of loan application by debtor (case study: Bank pasar of Yogyakarta special region)," in *Proc. 3rd Int. Conf. Inf. Commun. Technol. (ICoICT)*, May 2015, pp. 75–80.
[111] S. Ruggieri, "Efficient c4. 5 [classification algorithm]," *IEEE Trans. Knowl. Data Eng.*, vol. 14, no. 2, pp. 438–444, Aug. 2002.
[112] G. Ke, Q. Meng, T. Finley, T. Wang, W. Chen, W. Ma, Q. Ye, and T.-Y. Liu, "LightGBM: A highly efficient gradient boosting decision tree," in *Proc. Adv. Neural Inf. Process. Syst.*, 2017, pp. 3146–3154.
[113] C. M. Biship, *Pattern Recognition and Machine Learning*, vol. 4, no. 4. New York, NY, USA: Springer, 2006.
[114] Y. Freund and R. E. Schapire, "Experiments with a new boosting algorithm," in *Proc. Int. Conf. Mach. Learn.*, vol. 96, 1996, pp. 148–156.
[115] H. Drucker, D. Wu, and V. N. Vapnik, "Support vector machines for spam categorization," *IEEE Trans. Neural Netw.*, vol. 10, no. 5, pp. 1048–1054, 1999.
[116] A. Cevik and I. H. Guzelbey, "Neural network modeling of strength enhancement for CFRP confined concrete cylinders," *Building Environ.*, vol. 43, no. 5, pp. 751–763, May 2008.
[117] S. S. Al-jaboriy, N. N. A. Sjarif, S. Chuprat, and W. M. Abduallah, "Acute lymphoblastic leukemia segmentation using local pixel information," *Pattern Recognit. Lett.*, vol. 125, pp. 85–90, Jul. 2019.
[118] H.-S. Park and C.-H. Jun, "A simple and fast algorithm for K-medoids clustering," *Expert Syst. Appl.*, vol. 36, no. 2, pp. 3336–3341, Mar. 2009.
[119] S. Mitra, H. Banka, and W. Pedrycz, "Rough–fuzzy collaborative clustering," *IEEE Trans. Syst., Man, Cybern., B, Cybern.*, vol. 36, no. 4, pp. 795–805, Aug. 2006.
[120] P. Viswanathan, "Fuzzy C means detection of leukemia based on morphological contour segmentation," *Proc. Comput. Sci.*, vol. 58, pp. 84–90, Jan. 2015.
[121] S. Mohapatra, D. Patra, and S. Satpathy, "An ensemble classifier system for early diagnosis of acute lymphoblastic leukemia in blood microscopic images," *Neural Comput. Appl.*, vol. 24, nos. 7–8, pp. 1887–1904, 2014.
[122] M.-C. Su, "Use of neural networks as medical diagnosis expert systems," *Comput. Biol. Med.*, vol. 24, no. 6, pp. 419–429, Nov. 1994.
[123] R. A. Hazarika, A. Abraham, D. Kandar, and A. K. Maji, "An improved LeNet-deep neural network model for Alzheimer's disease classification using brain magnetic resonance images," *IEEE Access*, vol. 9, pp. 161194–161207, 2021.
[124] I. Domingues, I. L. Sampaio, H. Duarte, J. A. M. Santos, and P. H. Abreu, "Computer vision in esophageal cancer: A literature review," *IEEE Access*, vol. 7, pp. 103080–103094, 2019.
[125] J. Yosinski, J. Clune, Y. Bengio, and H. Lipson, "How transferable are features in deep neural networks?" in *Proc. Adv. Neural Inf. Process. Syst.*, 2014, pp. 3320–3328.
[126] M. Claro, L. Vogado, R. Veras, A. Santana, J. Tavares, J. Santos, and V. Machado, "Convolution neural network models for acute leukemia diagnosis," in *Proc. Int. Conf. Syst., Signals Image Process. (IWSSIP)*, Jul. 2020, pp. 63–68.
[127] C. Szegedy, W. Liu, Y. Jia, P. Sermanet, S. Reed, D. Anguelov, D. Erhan, V. Vanhoucke, and A. Rabinovich, "Going deeper with convolutions," in *Proc. IEEE Conf. Comput. Vis. Pattern Recognit. (CVPR)*, Jun. 2015, pp. 1–9.
[128] A. G. Howard, M. Zhu, B. Chen, D. Kalenichenko, W. Wang, T. Weyand, M. Andreetto, and H. Adam, "MobileNets: Efficient convolutional neural networks for mobile vision applications," 2017, *arXiv:1704.04861*.
[129] M. Sandler, A. Howard, M. Zhu, A. Zhmoginov, and L.-C. Chen, "MobileNetV2: Inverted residuals and linear bottlenecks," in *Proc. IEEE/CVF Conf. Comput. Vis. Pattern Recognit.*, Jun. 2018, pp. 4510–4520.
[130] F. Chollet, "Xception: Deep learning with depthwise separable convolutions," in *Proc. IEEE Conf. Comput. Vis. Pattern Recognit. (CVPR)*, Jul. 2017, pp. 1251–1258.
[131] X. Zhang, X. Zhou, M. Lin, and J. Sun, "ShuffleNet: An extremely efficient convolutional neural network for mobile devices," in *Proc. IEEE Conf. Comput. Vis. Pattern Recognit.*, Jun. 2018, pp. 6848–6856.
[132] Y. LeCun, L. Bottou, Y. Bengio, and P. Haffner, "Gradient-based learning applied to document recognition," *Proc. IEEE*, vol. 86, no. 11, pp. 2278–2324, Nov. 1998.
[133] P. K. Mallick, S. K. Mohapatra, G.-S. Chae, and M. N. Mohanty, "Convergent learning–based model for leukemia classification from gene expression," *Pers. Ubiquitous Comput.*, vol. 2, pp. 1–8, Oct. 2020.
[134] A. Genovese, M. S. Hosseini, V. Piuri, K. N. Plataniotis, and F. Scotti, "Acute lymphoblastic leukemia detection based on adaptive unsharpening and deep learning," in *Proc. IEEE Int. Conf. Acoust., Speech Signal Process. (ICASSP)*, Jun. 2021, pp. 1205–1209.
[135] C. Mondal, M. K. Hasan, M. T. Jawad, A. Dutta, M. R. Islam, M. A. Awal, and M. Ahmad, "Acute lymphoblastic leukemia detection from microscopic images using weighted ensemble of convolutional neural networks," 2021, *arXiv:2105.03995*.
[136] J. Redmon, S. Divvala, R. Girshick, and A. Farhadi, "You only look once: Unified, real-time object detection," in *Proc. IEEE Conf. Comput. Vis. Pattern Recognit.*, Jun. 2016, pp. 779–788.
[137] J. Redmon and A. Farhadi, "YOLO9000: Better, faster, stronger," in *Proc. IEEE Conf. Comput. Vis. Pattern Recognit.*, Jul. 2017, pp. 7263–7271.
[138] J. Redmon and A. Farhadi, "YOLOv3: An incremental improvement," 2018, *arXiv:1804.02767*.
[139] A. Bochkovskiy, C.-Y. Wang, and H.-Y. Mark Liao, "YOLOv4: Optimal speed and accuracy of object detection," 2020, *arXiv:2004.10934*.
[140] R. Al-Qudah and C. Y. Suen, "Synthetic blood smears generation using locality sensitive hashing and deep neural networks," *IEEE Access*, vol. 8, pp. 102530–102539, 2020.
[141] R. Khandekar, P. Shastry, S. Jaishankar, O. Faust, and N. Sampathila, "Automated blast cell detection for acute lymphoblastic leukemia diagnosis," *Biomed. Signal Process. Control*, vol. 68, Jul. 2021, Art. no. 102690.
[142] S. Gehlot, A. Gupta, and R. Gupta, "SDCT-AuxNet: DCT augmented stain deconvolutional CNN with auxiliary classifier for cancer diagnosis," *Med. Image Anal.*, vol. 61, Apr. 2020, Art. no. 101661.
[143] R. Duggal, A. Gupta, R. Gupta, and P. Mallick, "SD-layer: Stain deconvolutional layer for CNNs in medical microscopic imaging," in *Proc. Int. Conf. Med. Image Comput.-Assist. Intervent*. Springer, 2017, pp. 435–443.
[144] S. Gehlot, A. Gupta, and R. Gupta, "A CNN-based unified framework utilizing projection loss in unison with label noise handling for multiple myeloma cancer diagnosis," *Med. Image Anal.*, vol. 72, Aug. 2021, Art. no. 102099.
[145] M. Schuster and K. K. Paliwal, "Bidirectional recurrent neural networks," *IEEE Trans. Signal Process.*, vol. 45, no. 11, pp. 2673–2681, Nov. 1997.
[146] S. Hochreiter and J. Schmidhuber, "Long short-term memory," *Neural Comput.*, vol. 9, no. 8, pp. 1735–1780, 1997.
[147] M.-H. Su, C.-H. Wu, K.-Y. Huang, and T.-H. Yang, "Cell-coupled long short-term memory with *L*-skip fusion mechanism for mood disorder detection through elicited audiovisual features," *IEEE Trans. Neural Netw. Learn. Syst.*, vol. 31, no. 1, pp. 124–135, Mar. 2020.
[148] S. Shah, W. Nawaz, B. Jalil, and H. A. Khan, "Classification of normal and leukemic blast cells in b-all cancer using a combination of convolutional and recurrent neural networks," in *C-NMC Challenge: Classification in Cancer Cell Imaging*. Singapore: Springer, 2019, pp. 23–31.
[149] I. Goodfellow, Y. Bengio, and A. Courville, *Deep Learning*. Cambridge, MA, USA: MIT Press, 2016.

[150] R. Gupta, S. Gehlot, and A. Gupta, "C-NMC: B-lineage acute lymphoblastic leukaemia: A blood cancer dataset," *Med. Eng. Phys.*, vol. 103, May 2022, Art. no. 103793.
[151] G. Jothi, H. H. Inbarani, A. T. Azar, and K. R. Devi, "Rough set theory with Jaya optimization for acute lymphoblastic leukemia classification," *Neural Comput. Appl.*, vol. 31, no. 9, pp. 5175–5194, Sep. 2019.
[152] L. H. S. Vogado, R. D. M. S. Veras, A. R. Andrade, R. R. V. E. Silva, F. H. D. De Araujo, and F. N. S. De Medeiros, "Unsupervised leukemia cells segmentation based on multi-space color channels," in *Proc. IEEE Int. Symp. Multimedia (ISM)*, Dec. 2016, pp. 451–456.
[153] A. S. A. Nasir, M. Y. Mashor, and H. Rosline, "Unsupervised colour segmentation of white blood cell for acute leukaemia images," in *Proc. IEEE Int. Conf. Imag. Syst. Techn.*, May 2011, pp. 142–145.
[154] P. Kumar and S. Vasuki, "Automated diagnosis of acute lymphocytic leukemia and acute myeloid leukemia using multi-sv," *J. Biomed. Imag. Bioeng.*, vol. 1, no. 1, pp. 20–24, 2017.
[155] S. Goswami, S. Mehta, D. Sahrawat, A. Gupta, and R. Gupta, "Heterogeneity loss to handle intersubject and intrasubject variability in cancer," 2020, *arXiv:2003.03295*.
[156] A. Gupta and R. Gupta, *C-NMC Challenge: Classification in Cancer Cell Imaging*, vol. 10. Singapore: Springer, 2019, pp. 978–981.

PRADEEP KUMAR DAS (Graduate Student Member, IEEE) received the B.Tech. degree in electronics and telecommunication engineering from the Biju Patnaik University of Technology (BPUT), Odisha, India, in 2013, and the M.Tech. degree in electronics and telecommunication engineering from the Veer Surendra Sai Unversity of Technology (VSSUT), Burla, India, in 2017. He is currently pursuing the Ph.D. degree in electronics and communication engineering with the National Institute of Technology Rourkela (NIT Rourkela). His research interests include computer vision, medical image processing, machine learning, deep learning, and signal processing. He has published several Elsevier and IEEE journals IEEE TRANSACTIONS. He is an Active Reviewer in several IEEE journals and IEEE TRANSACTIONS, such as IEEE TRANSACTIONS ON CYBERNETICS, IEEE TRANSACTIONS ON SYSTEMS, MAN, AND CYBERNETICS: SYSTEMS, IEEE TRANSACTIONS ON CIRCUITS AND SYSTEMS FOR VIDEO TECHNOLOGY, IEEE TRANSACTIONS ON EMERGING TOPICS IN COMPUTATIONAL INTELLIGENCE, and IEEE ACCESS.

DIYA V A (Graduate Student Member, IEEE) received the B.Tech. degree in electronics and communication engineering from the Government Engineering College, Thrissur, Kerala, in 2018, and the M.Tech. degree in electronics and communication engineering from the National Institute of Technology Rourkela (NIT Rourkela), in 2021. Her research interests include image processing, machine learning, deep learning, and medical image analysis.

SUKADEV MEHER (Member, IEEE) received the B.Sc. (Engg.) degree in electronics and communication engineering from the University College of Engineering (UCE), Burla, India, in 1984, the M.E. degree in electronics systems and communication engineering from the Regional Engineering College, Rourkela, India, in 1992, and the Ph.D. degree in electronics engineering and image processing from the National Institute of Technology Rourkela (NIT Rourkela), in 2005. He is currently a Professor with the Department of Electronics and Communication Engineering, NIT Rourkela. He has been assuming this position, since July 2011. He has over 100 papers in international/national journals and conferences. His Google Scholar H-index is 17 with more than 1300 citations. His research interests include image processing, signal processing, medical image processing, deep learning, and machine learning.

RUTUPARNA PANDA (Member, IEEE) was born in 1963. He received the B.Sc. (Engg.) and M.Sc. (Engg.) degrees from UCE Burla, in 1985 and 1988, respectively, and the Ph.D. (Engg.) degree from IIT, KGP, in 1998. He is currently a Professor with the Department of Electronics and Telecommunication Engineering, VSS University of Technology, Burla. He was the Former HOD of ECE, the HOD of CSE, the Dean of Academic Affairs, the Dean of SRIC, and the Dean of Continuing Education Program. He has guided 35 M.Tech. Theses and eight Ph.D. Theses. He has published over 150 papers in international/national journals and conferences. He has more than 2000 academic citations with H-index of 26 and i10-index of 48 as per google scholar. He is the coauthor of a book titled *AI Techniques for Biomedical Engineering Applications* and eight book chapters. He is currently serving as an Associate Editor for *Engineering Applications of Artificial Intelligence* (EAAI). He is a reviewer of many reputed international journals, such as IEEE TRANSACTIONS and Elsevier journals. He received Highly Cited Research Award, in December 2016, *Swarm and Evolutionary Computation* journal (Elsevier). He received Certificate of Appreciation Award for *Quality Research Journal* Publications for the year 2020 from the VSS University of Technology. His research interests include digital signal/image processing, bioinformatics, biomedical engineering, VLSI signal processing, soft computing, machine intelligence, and AI.

AJITH ABRAHAM (Senior Member, IEEE) received the Master of Science degree from Nanyang Technological University, Singapore, in 1998, and the Ph.D. degree in computer science from Monash University, Melbourne, Australia, in 2001. He is currently the Director of the Machine Intelligence Research Laboratories (MIR Laboratories), a Not-for-Profit Scientific Network for Innovation and Research Excellence Connecting Industry and Academia. The Network with HQ in Seattle, USA, is currently more than 1,500 scientific members from over 105 countries. As an Investigator/a Co-Investigator, he has won research grants worth over more than 100 Million U.S. Dollar. He currently holds two university professorial appointments. He works as a Professor in artificial intelligence with Innopolis University, Russia, and the Yayasan Tun Ismail Mohamed Ali Professorial Chair of Artificial Intelligence with UCSI, Malaysia. He works in a multi-disciplinary environment and he has authored/co-authored more than 1,400 research publications out of which there are more than 100 books covering various aspects of computer science. One of his books was translated to Japanese and a few other articles were translated to Russian and Chinese. He has more than 46,000 academic citations (H-index of more than 102 as Per Google Scholar). He has given more than 150 plenary lectures and conference tutorials (in more than 20 countries). He was the Chair of IEEE Systems Man and Cybernetics Society Technical Committee on Soft Computing (which has over more than 200 members), from 2008 to 2021, and served as a Distinguished Lecturer for IEEE Computer Society representing Europe, from 2011 to 2013. He was the Editor-in-Chief of *Engineering Applications of Artificial Intelligence* (EAAI), from 2016 to 2021 and serves/served the editorial board of over 15 international journals indexed by Thomson ISI.